REPORT 1322

METHOD FOR CALCULATING THE AERODYNAMIC LOADING ON AN OSCILLATING FINITE WING IN SUBSONIC AND SONIC FLOW [1]

By Harry L. Runyan and Donald S. Woolston

SUMMARY

This report presents a method for determining the air forces on an oscillating finite wing of general plan form in subsonic flow including the limiting case of sonic flow. The method utilizes some of the concepts developed by Falkner (British R. & M. No. 1910) for steady lifting-surface theory. The loading on the wing is assumed to be given by a series containing unknown coefficients which satisfies various boundary conditions at the edges. The required integrations are performed by approximate means, and a set of simultaneous equations in terms of the coefficients in the loading series is obtained. Solution of this set of equations then gives the loading coefficients. The method is applied to rectangular and delta wings and comparison is made with existing theory. A sample calculation is given in an appendix.

INTRODUCTION

The analytical determination of the air forces on oscillating wings has been a continuing problem for over 30 years. Most of the effort has been directed toward the determination of the forces on wings in two-dimensional flow, and results have been obtained for a complete range of Mach numbers, both subsonic and supersonic. For finite wings, however, the analytical work is still in a state of development for all speed ranges. The main effort has been directed toward the incompressible case (for example, refs. 1 to 8) and the supersonic field (refs. 9 to 14) leaving an important area virtually untouched, namely, the subsonic range of Mach numbers between 0 and 1. Among the few studies that have been made in this range of Mach numbers have been those of Merbt and Landahl (ref. 15), who extended some of the work at very low aspect ratio to include the effect of Mach number, and the work of Voss, Zartarian, and Hsu (ref. 16). In addition, Reissner (ref. 17) made a preliminary assessment of the use of Mathieu functions for subsonic compressible flow, and W. P. Jones (ref. 18) and Lehrian (ref. 19) studied the cases for larger aspect ratios. The present report deals with some recent efforts which have been made toward filling this gap, namely the development of a wing-surface theory for subsonic and sonic flow.

In the stationary two-dimensional case, the effects of compressibility may readily be obtained from results of incompressible theory by application of simple transformation or correction factors such as the well-known Prandtl-Glauert factor. In the stationary three-dimensional case, the effect of compressibility may be treated as an extension of the two-dimensional procedure in a simple manner as proposed by Göthert (ref. 20). In a further extension for the oscillating compressible case, Miles (ref. 21) has proposed a method involving several transformation steps for correcting the results of incompressible theory to include the effects of compressibility for a finite wing. The method is, however, restricted to low values of the reduced frequency. It therefore appears to be necessary to deal with the boundary-value problem directly in order to provide a method of general applicability which may be used, for example, in flutter work.

The linearized boundary-value problem for the oscillating finite wing in a compressible flow may be approached from two points of view. One approach involves the transformation of the governing differential equation by a suitable choice of coordinates followed by the use of the classical method of separation of variables. Solutions are then found in terms of series of orthogonal functions. This method was used by Schade and Krienes (ref. 22) in obtaining solutions for the oscillating circular plate and has recently been generalized by Kuessner (ref. 23). It has been pointed out that there is a definite limit to the number of generalized coordinate systems appropriate to the wave equation and to the corresponding orthogonal functions available. The method is, therefore, limited to specialized plan forms such as the circular or the elliptic plate.

The second approach involves a direct consideration of the integral equation relating pressure and downwash. The integral equation may be derived from the standpoint of either the velocity potential or the acceleration potential. Inasmuch as one is primarily interested in the pressures on the wing surface, it seems more direct to use the form of the integral equation associated with the pressure, namely, the acceleration potential approach; therefore, this procedure is used in the present report.

Basic to the solution of the integral equation is the evaluation of its kernel, a function which represents the downwash at a point in the plane of the wing due to a unit loading. Only recently (ref. 24), the kernel function for oscillating finite wings in subsonic and sonic flow has been reduced to a form which can be conveniently evaluated. This background of available information on the kernel has led to the consideration of numerical approaches for handling the integral equation in the development of general lifting-surface methods which could be used for any speed range.

[1] Supersedes NACA Technical Note 3694 by Harry L. Runyan and Donald S. Woolston, 1956.

A similar integral equation appears in the steady case, but involves a much simpler kernel function and a number of approximate solutions have been successfully developed. In selecting an approximate method for handling the integral equation in the oscillatory case, the various procedures developed for the steady case were examined. In considering these procedures, it was kept in mind that a lifting-surface theory which is to be used for flutter calculations must meet certain requirements beyond those usually considered in the steady case. One essential requirement is that not only the lift but also the moment must be accurately predicted. In several of the methods now being used for the steady case, the wing is essentially replaced by a single line at the ¼-chord position. This placement essentially fixes the center of pressure at the ¼ chord, and thus the moment is constrained to become a function only of the lift force. In the case of an airplane of normal configuration with a tail placed a considerable distance from the wing, the contribution of the wing pitching moment is very small compared with the pitching moment due to the tail. However, for tailless configurations and for aeroelastic problems such as flutter, the moment on the wing is of predominant importance and must be accurately predicted.

In addition to the previously mentioned requirement of predicting the moment, the method should be easily adaptable to the calculation of the loading on oscillating flexible wings and, in addition, should take into account the effects of compressibility. It appeared that, among others, a method developed for the steady incompressible case by Falkner (ref. 25) could be extended to include these requirements and this method was selected as the basis for the present investigation.

Among other methods considered was a multiple-line approach suggested by the procedure of Schlichting and Kahlert (ref. 26) for the case of steady flow. The procedure is thought to be of interest in that it indicates a simpler alternative means of handling the lifting-surface problems. An extension of this method to the oscillatory case is also made in the present investigation.

The primary aim of the present investigation has been the development of a lifting-surface method for calculating the forces on a wing of any plan form which is harmonically oscillating in a subsonic or sonic flow. The method uses some of the concepts of Falkner in an extension to the compressible oscillating case. First, a brief description of the basic integral equation and some of the possible means of solution are given. Then, the basic theory of the method is given in detail in the body of the report, and the results of some calculations are shown for rectangular and delta wings. In appendix A, the numerical details of calculating the forces on a rectangular wing are given as an example. In appendix B, a treatment is given for certain integrals which arise in the method and which contain singularities. In appendix C the expression for the pitching moment for a delta wing is obtained. Finally, in appendix D, a description and some results of applying a multiple-line approach, based on a procedure used by Schlichting and Kahlert for steady flow, are given.

SYMBOLS

A	aspect ratio
a	axis of rotation measured from midchord in terms of half-chord, positive aft
a_{nm}	coefficients in expression for loading
b	half-chord, ft
$C_{L,q}$	lift coefficient associated with a degree of freedom q
$C_{M,q}$	moment coefficient associated with a degree of freedom q
c	chord, ft
$F(M)=-\frac{\beta}{2\pi}$	
F_{rN}	nondimensional downwash factor defined by equation (29)
$f_n(\xi)$	chordwise loading function
$G(M)=\frac{1}{2\pi\beta}$	
G_{r0},G_{rn}	chordwise replacement loads
$g_m(\eta),g_m(\mu)$	spanwise loading functions
$K\left[M,\frac{\omega}{V}(x-\xi),\frac{\omega}{V}(y-\eta)\right]$	kernel of three-dimensional integral equation
$\overline{K}(M,Z)$	kernel of two-dimensional integral equation, $\overline{K}(M,Z)=\int_{-\infty}^{\infty}K\left[M,\frac{\omega}{V}(x-\xi),\frac{\omega}{V}(y-\eta)\right]d\eta$
$\underline{K}$	nondimensional three-dimensional kernel defined by equation (28)
k	reduced-frequency parameter based on half-chord, $b\omega/V$
$\bar{k}$	reduced-frequency parameter based on ϵ, $\bar{k}=\frac{\epsilon\omega}{V}$
L_q	total lift on wing, associated with a degree of freedom q, lb
l	reference length
M	Mach number
M_q	moment about a, associated with a degree of freedom q, ft-lb
n,m,j	integers
q	dynamic pressure, $\frac{1}{2}\rho V^2$
$R_1=\sqrt{(x-\xi)^2+\beta^2(y+1)^2}$	
$R_2=\sqrt{(x-\xi)^2+\beta^2(y-1)^2}$	
S	area of wing surface
s	semispan of wing, ft
t	time
V	stream velocity
$w(x,y,t)$	vertical induced velocity or downwash
x,y,z,ξ,η	rectangular coordinates
x_g	control-point location
$x_o=(x-x_r)$	
x_r	chordwise coordinate for replacement loads

y_N	distance from control point to center of segment
$y_o=y-\eta$	
y'_L, y'_R	distances from a control point to midpoints of load segments located, respectively, to the left and right of the wing midspan, referred to ϵ
$Z=k(x_g-\xi)$ or $k(x_g-x_r)$	
α	generalized coordinate of an angular displacement
$\beta=\sqrt{1-M^2}$	
$\Gamma(\xi,\eta)$	vorticity distribution
$\Delta P_r(\mu)$	loading function defined by equation (26)
$\Delta p(\xi,\eta)$	pressure difference
δ	thickness ratio
ϵ	semispan of spanwise load segment, $s/20$, ft
θ	angular chordwise coordinate, $x=-\cos\theta$
λ	variable of integration
ρ	air density
Φ	angular spanwise coordinate, $\eta=-\cos\Phi$
ϕ	phase angle between lift or moment and position
ω	circular frequency, radians/sec
Subscript:	
q	denotes a degree of freedom (for pitch, $q=\alpha$)

DISCUSSION OF INTEGRAL EQUATION AND METHODS OF SOLUTION

The determination of the aerodynamic forces on an oscillating wing is a problem which, in general, must be handled by approximate or iterative procedures. In the two-dimensional case one approach to the problem has been the transformation of the governing differential equation and its associated boundary conditions to an integral equation for which approximate solutions can be found. It is interesting to note that for this two-dimensional case, an iterative solution based on the integral-equation approach preceded a more exact solution based on a series of Mathieu functions by about ten years.

In the case of wings of finite span, a transformation similar to that made in the two-dimensional case and leading to an integral equation can be made. The integral equation may be derived on the basis of the velocity potential or on the basis of the acceleration potential. The advantage of the use of the acceleration potential rests in the fact that the trailing surface of discontinuity is not explicitly introduced into the problem and the integral equation relates directly the downwash and the pressure difference on the wing. The disadvantage of the acceleration potential as compared with the velocity-potential approach lies in the appearance of a more complicated kernel of the integral equation.

INTEGRAL EQUATION

For compressible flow, the integral equation as derived on the basis of the acceleration potential and given, for example, in reference 24 may be written as

$$\frac{w(x,y,t)}{V}=\frac{1}{8\pi}\iint_S \frac{\Delta p(\xi,\eta)}{q} K\left[M, \frac{\omega}{V}(x-\xi), \frac{\omega}{V}(y-\eta)\right] d\xi\, d\eta \tag{1}$$

where w is the known vertical induced velocity or downwash, $\Delta p(\xi,\eta)$ is the loading or pressure difference (positive upward) at a point (ξ,η) on the wing surface, V is the stream velocity, and K is the kernel of the integral equation. The pressure difference $\Delta p(\xi,\eta)$ is related to the bound vorticity through the equation

$$\Delta p(\xi,\eta)=\rho V\Gamma(\xi,\eta)$$

so that equation (1) is sometimes written with $\frac{\Delta p(\xi,\eta)}{q}$ replaced by $\frac{2\Gamma(\xi,\eta)}{V}$. The function K represents, physically, the contribution to the downwash at a field point (x,y) in the plane of the wing due to a unit pressure difference at a loading point (ξ,η) also located in the plane of the wing.

The kernel K is discussed in reference 24 and appears originally in an integral form as

$$K\left[M, \frac{\omega}{V}(x-\xi), \frac{\omega}{V}(y-\eta)\right]$$

$$=\lim_{z\to 0}\frac{\partial^2}{\partial z^2} e^{-i\frac{\omega}{V}(x-\xi)}\int_{-\infty}^{x-\xi} \frac{e^{i\frac{\omega}{V\beta^2}\left[\lambda-M\sqrt{\lambda^2+\beta^2(y-\eta)^2+\beta^2z^2}\right]}}{\sqrt{\lambda^2+\beta^2(y-\eta)^2+\beta^2z^2}}\, d\lambda \tag{2}$$

where ω is the circular frequency of the oscillating wing.

In the form given by equation (2), the kernel function appears as an improper integral whose complete integration in closed form has not been accomplished. The kernel function has been extensively treated in reference 24, however, and has been reduced to a form which can be evaluated. The reduced form of the kernel given in reference 24 contains Bessel and Struve functions and proper nonsingular integrals which can be handled by numerical means. The kernel contains singularities at $y-\eta=0$ and $x-\xi\geqq 0$, but these singularities have been isolated and expressed in a form which can be handled in numerical procedures. Also given in reference 24 is an expansion of the kernel into a series in powers of the reduced frequency, which for the present time serves as the most practical form for application of the kernel.

The solution of equation (1) requires a determination of the unknown loading distribution $\Delta p(\xi,\eta)$ subject to known boundary conditions. In view of the complicated nature of the kernel, an exact analytical solution of equation (1) does not seem possible. It appears necessary, therefore, to consider some numerical method of solution and several possible approximate methods are discussed in the next section.

SOME APPROXIMATE PROCEDURES

In searching for an approximate means of handling the integral equation, two approaches seem likely, one involving an approximation for the kernel and the other an approximation for the loading. The first of these would involve a replacement of the complicated kernel function by a simpler function which behaves in a similar manner (with regard to singularities, and so forth) but with which the integral equation could be inverted and solved analytically for the unknown loading. Such a procedure has been used by Fettis (ref. 27) for the two-dimensional, subsonic, oscillatory case and, in part, by Lawrence (ref. 28) for the finite wings in incompressible steady flow and by Lawrence and Gerber (ref. 29) for oscillating finite wings in incompressible flow. The application of such a procedure to the case of compressible flow would be quite difficult, but is perhaps worthy of further consideration.

A second possible approach involves leaving the kernel unchanged and selecting an appropriate expression for the loading which leaves only certain unknown coefficients to be determined. By such a procedure the integral equation can be reduced to a sum of definite integrals and the unknown constants can be determined by collocation, that is, by forcing the solution to fit the known downwash conditions at a number of points on the surface. Although difficulties arise in the integrations because of singularities in the kernel and the loading, they can be handled in numerical methods. Various forms of this procedure have been used quite successfully for oscillating two-dimensional wings and for finite wings in steady flow.

A logical extension of this second approach, the choice of a replacement function for the loading, to the three-dimensional problem would involve finding a means of handling the definite integrals which arise. It would seem possible to divide the wing into many small areas and, with an assumed form of the loading on each area, integrate numerically over each area to find the downwash at a point on the surface. Such a procedure would lead, however, to a system of equations in the unknown constants of at least the order of the number of areas so that lengthy computations would arise which would require computing equipment of great capacity.

In searching for a less cumbersome method, it is natural to study the possibility of utilizing some of the concepts of procedures which have already been developed for the case of steady flow. Several methods for steady flow seem adaptable to the unsteady problem. Among those to be considered are the procedures of Falkner (ref. 25), Multhopp (ref. 30), Weissinger (ref. 31), and Schlichting and Kahlert (ref. 26). A brief discussion of these methods in relation to the objectives of the present investigation is given subsequently.

The methods developed for the steady case by Falkner and by Multhopp represent attempts at lifting-surface procedures for handling the integral equation. In both approaches, the unknown loading is expressed in terms of a series of chosen modes of loading with unknown coefficients to be determined by collocation. In both methods, also, the double integrations are performed numerically and lead to sets of downwash factors. It appears that either method could be extended to the unsteady case and systematized through the development of suitable tables of the downwash factors. For the purpose of extending such procedures to the unsteady-flow problem, in the present investigation, the Falkner procedure has been considered preferable since considerably fewer tabulations are required. The development of a lifting-surface approach based on the method of Falkner is the main objective of this report. An extension of the steady-state procedure of Multhopp to the oscillatory case has been performed by Jordan and some results are given in reference 32.

It should be noted that W. P. Jones (refs. 2 and 18) has also treated the problem of determining the aerodynamic forces on wings of any plan form by using some of Falkner's concepts. The method differs from the one to be presented in this report and pursues a different numerical path since in the Jones procedure the basic integral equation was treated on the basis of the concept of the velocity potential. The use of the velocity potential results in a double integration over the entire field of velocity discontinuity, that is, over the wing and its wake. The use of the acceleration potential, employed in this report, involves a double integration only over the area of pressure discontinuity, that is, over the wing surface itself, since no pressure discontinuity exists in the wake.

Other steady-state procedures mentioned previously were those of Schlichting and Kahlert and of Weissinger. These methods represent lifting-line rather than lifting-surface approaches. In the Weissinger method a single lifting line is placed at the ¼-chord position on the surface and the known downwash is satisfied at points on the ¾-chord position. The Schlichting procedure makes use of several lifting lines. The surface is divided into a number of spanwise strips of equal chord. A lifting line is placed at the ¼-chord position of each strip and the downwash conditions are satisfied at points on the ¾-chord position of each strip. Since a lifting-line procedure might be expected to involve less labor than a lifting-surface approach, an attempt was made in the present study to extend the Schlichting method to the case of unsteady flow. The application of the Schlichting approach to the oscillating case is discussed in appendix D.

In the following two sections the lifting-surface method of the present report is developed, first for the case of subsonic flow and then for the limiting case of $M=1$.

DESCRIPTION OF SURFACE-LOADING METHOD FOR SUBSONIC FLOW

The solution of the integral equation for the case of an oscillating three-dimensional wing involves a double integration over the plan form of the wing as indicated by equation (1):

$$\frac{w(x,y,t)}{V}=\frac{1}{8\pi q}\iint_S \Delta p(\xi,\eta)K\left[M,\frac{\omega}{V}(x-\xi),\frac{\omega}{V}(y-\eta)\right]d\xi\,d\eta$$

Of the three main ingredients of the problem—the downwash,

the kernel, and the loading—which are related by this equation, two can be considered as known. The kernel function K can be evaluated through the use of the forms given in reference 24. The downwash $w(x,y,t)$ is determined by the motion of the airfoil. This leaves as the only unknown in equation (1) the function $\Delta p(\xi,\eta)$, the magnitude of the loading at points (ξ,η) of the surface.

STATEMENT OF THE BOUNDARY CONDITIONS FOR THE DOWNWASH

For linearized flow, the downwash function $w(x,y,t)$ can be determined from the motion of the mean surface of the airfoil through the relation

$$w(x,y,t)=\frac{\partial}{\partial t}f(x,y,t)+V\frac{\partial}{\partial x}f(x,y,t) \tag{3a}$$

where, for harmonic motion,

$$f(x,y,t)=\bar{f}(x,y)e^{i\omega t}$$

so that $\bar{f}(x,y)$ is the amplitude of the displacement of the mean surface from the equilibrium position. Once an appropriate function for $\bar{f}(x,y)$ is chosen, the downwash is known and the loading can be determined from equation (1). For the usual modal type of flutter analysis, for example, $\bar{f}(x,y)$ could be found from the assumed vibration modes of the structure.

Because the basic problem of determining the loading for a given downwash as expressed by equation (1) is linear, it is often convenient to consider the problem separated into a sum of individual problems, each associated with a particular selected type of motion or degree of freedom and, hence, with a particular downwash function. This implies that the total downwash can be written as a sum of individual downwash functions, so that equation (3a) appears as

$$\begin{aligned} w(x,y,t)&=\left(\frac{\partial}{\partial t}+V\frac{\partial}{\partial x}\right)[\bar{f}_1(x,y)+\bar{f}_2(x,y)+\ \ldots\ +\bar{f}_q(x,y)]e^{i\omega t}\\ &=[w_1(x,y)+w_2(x,y)+\ \ldots\ +w_q(x,y)]e^{i\omega t} \end{aligned} \tag{3b}$$

where $w_q(x,y)$ is the downwash associated with the particular degree of freedom $\bar{f}_q(x,y)$. The basic problem of this report is then the determination of the loading $\Delta p_q(\xi,\eta)$ associated with any one of the downwash factors $w_q(x,y)$.

TREATMENT OF THE LOADING

In addition to the downwash conditions set by equations (3), the loading $\Delta p(\xi,\eta)$ must satisfy various conditions at the edges of the plan form. In the chordwise direction, for subsonic flow, the loading must be infinite at the leading edge and vanish, in accordance with the Kutta condition, at the trailing edge. In the spanwise direction, the loading should become zero at the wing tips.

Series expression for the loading.—As a first step in the determination of the unknown loading, it is assumed that the function $\Delta p(\xi,\eta)$ can be expressed in terms of a series of both spanwise and chordwise pressure or loading modes, so chosen as to satisfy the edge conditions just discussed and containing arbitrary coefficients to be determined. The spanwise modes are expressed in terms of the variable η. It is convenient to express the chordwise pressure modes in terms of an often used variable θ, related to ξ and based on the circular cylinder enveloping each chord as diameter and shown by sketch 1 and in equation (4).

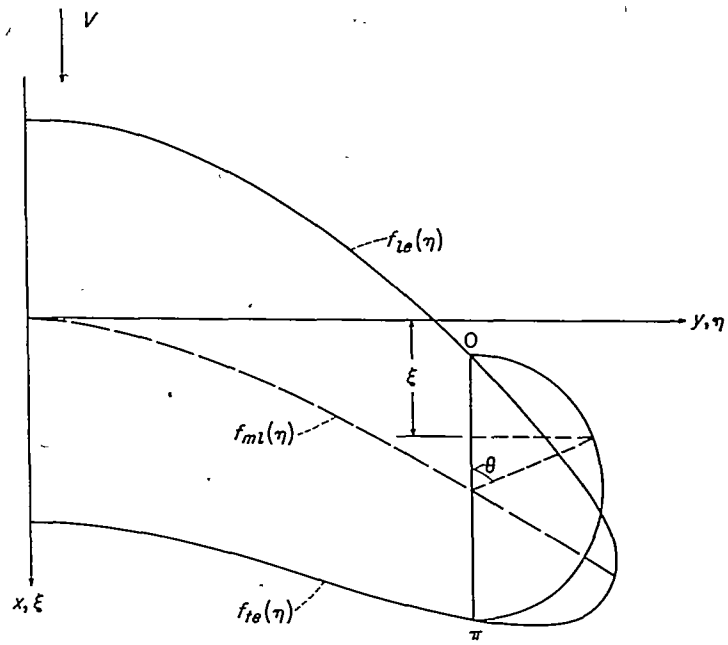

Sketch 1.

$$\xi=f_{ml}(\eta)-b(\eta)\cos\theta \tag{4}$$

where

$$b(\eta)=\frac{1}{2}[f_{te}(\eta)-f_{le}(\eta)]$$

In terms of the variables θ and η, the loading associated with a particular downwash distribution $w_q(x,y)$ may be expressed in terms of the summation of pressure modes and written as

$$\begin{aligned} \Delta p_q(\xi,\eta)=\frac{8\rho V^2}{2b(\eta)}\sqrt{s^2-\eta^2}\Big[&\cot\frac{\theta}{2}(a_{00}^q+a_{01}^q\eta+a_{02}^q\eta^2+\ \ldots\ )+\\ &\sin\theta(a_{10}^q+a_{11}^q\eta+a_{12}^q\eta^2+\ \ldots\ )+\sin 2\theta(a_{20}^q+a_{21}^q\eta+\\ &a_{22}^q\eta^2+\ \ldots\ )+\ \ldots\Big] \end{aligned} \tag{5a}$$

where the superscript q identifies a particular downwash.

The series form of the loading given by equation (5a) satisfies the Kutta condition ($\Delta p=0$ at the trailing edge) and has the desired type of singularity $1/\sqrt{x}$ where x is measured from the leading edge. The terms in η are of such a form as to cause $\Delta p(\xi,\eta)$ to become zero with infinite slope at the wing tips. The use of this series form for $\Delta p(\xi,\eta)$ means the pressure distribution is essentially synthesized by a series of chosen pressure modes and the values of a_{nm} determine the contribution of each pressure mode to the final pressure distribution.

Equation (5a) can be written in more concise form, as

$$\Delta p_q(\theta,\eta)=\frac{8\rho V^2}{2b(\eta)}\sum_{n=0}^{\infty}\sum_{m=0}^{\infty}a_{nm}^q f_n(\xi)g_m(\eta) \tag{5b}$$

where

$$\left.\begin{aligned} f_0(\xi)&=\cot\frac{\theta}{2} && (n=0)\\ f_n(\xi)&=\sin n\theta && (n\neq 0)\\ g_m(\eta)&=\eta^m\sqrt{s^2-\eta^2} \end{aligned}\right\} \tag{6}$$

(For symmetrical motions of a wing, $w_q(x,y)=w_q(x,-y)$, the odd terms in η need not be retained. For unsymmetrical motions, $w_q(x,y)=-w_q(x,-y)$, the even-powered terms in η do not have to be retained. In the numerical examples to be given in a later section, symmetric motions are considered.)

Illustrative expressions for the force and moment.—The specific problem is the determination of the coefficients a_{nm} in equation (5a) or (5b) and, as has been indicated, a particular set of values for a_{nm} must be found for each downwash $w_q(x,y)$. Once a set of values for a_{nm} has been determined, a particular loading $\Delta p_q(\xi,\eta)$ is defined by equation (5a) or (5b). This expression for $\Delta p_q(\xi,\eta)$ gives the pressure distribution and can be integrated to obtain various desired section forces or total forces. For example, total lift and moment coefficients associated with the motion $\bar{f}_q(x,y)$ can be found through the relations

$$\frac{L_q}{qS}=C_{L,q}=\frac{1}{qS}\iint_S \Delta p_q(\xi,\eta)d\xi\, d\eta \tag{7a}$$

and

$$\frac{M_q}{qSb}=C_{M,q}=\frac{1}{qSb}\iint_S (\xi-a)\Delta p_q(\xi,\eta)d\xi\, d\eta \tag{7b}$$

where the moment is obtained about a spanwise axis $\xi=a$.

By substituting equation (5a) into equation (7a) the following result for the lift coefficient is obtained which is valid for any plan form:

$$C_{L,q}=\frac{\pi^2 A}{16}(16a_{00}^q+8a_{10}^q+4a_{02}^q+2a_{12}^q+2a_{04}^q+a_{14}^q) \tag{8}$$

The expression for the moment about the axis considered must be determined for each particular plan form. The moment coefficient will take on a form similar to equation (8) but with constants determined by the plan-form geometry. For a rectangular wing, for example, the moment coefficient for moment about the midchord ($a=0$) is

$$C_{M,q}=-\frac{\pi^2 A}{32}(16a_{00}^q+4a_{02}^q+2a_{04}^q+8a_{20}^q+2a_{22}^q+a_{24}^q) \tag{9}$$

The equation for the moment coefficient for a delta-wing plan form is given in appendix C.

REPLACEMENT OF THE INTEGRAL EQUATION BY A SUMMATION OF DEFINITE INTEGRALS

In the rest of the analysis, it will be convenient to deal with a general downwash $w(x,y)$ and to drop the subscript and superscript q. In order to evaluate the coefficients a_{nm} for a particular downwash $w_q(x,y)$, the first step involves the substitution of the loading series (eq. (5a)) into the integral equation (eq. (1)) to give

$$\frac{w(x,y)}{V}=\frac{4\rho V^2}{8\pi qb}\iint_S\sqrt{s^2-\eta^2}\Big[\cot\frac{\theta}{2}(a_{00}+a_{01}\eta+a_{02}\eta^2+\ldots)+\sin\theta(a_{10}+a_{11}\eta+a_{12}\eta^2+\ldots)+\sin 2\theta(a_{20}+a_{21}\eta+a_{22}\eta^2+\ldots)+\ldots\Big]K\Big[M,\frac{\omega}{V}(x-\xi),\frac{\omega}{V}(y-\eta)\Big]d\xi\, d\eta \tag{10}$$

or if the form for $\Delta p(\xi,\eta)$ given by equation (5b) is used, the following is true:

$$\frac{w(x,y)}{V}=\frac{4\rho V^2}{8\pi qb}\sum_{n=0}^{\infty}\sum_{m=0}^{\infty}a_{nm}\iint_S f_n(\xi)g_m(\eta)K\Big[M,\frac{\omega}{V}(x-\xi),\frac{\omega}{V}(y-\eta)\Big]d\xi\, d\eta \tag{11}$$

A significant step toward the desired solution of the integral equation has now been arrived at because equation (10) or (11) is no longer an integral equation, that is, an unknown quantity no longer appears under an integral sign. Instead, the downwash $w(x,y)$ is now given by a summation of definite integrals multiplied by various unknown constants a_{nm}. These integrals are of the form

$$\left.\begin{aligned} &\iint_S \cot\frac{\theta}{2}\eta^m\sqrt{s^2-\eta^2}K\Big[M,\frac{\omega}{V}(x-\xi),\frac{\omega}{V}(y-\eta)\Big]d\xi\, d\eta\\ &\iint_S \sin n\theta\,\eta^m\sqrt{s^2-\eta^2}K\Big[M,\frac{\omega}{V}(x-\xi),\frac{\omega}{V}(y-\eta)\Big]d\xi\, d\eta \end{aligned}\right\} \tag{12}$$

The numerical evaluation of these integrals is an important part of the labor of the present method, for once their values have been calculated, one can proceed immediately to the determination of a_{nm} and, therefore, to the determination of the pressure distribution. In the method under consideration, the required integrations are performed numerically. Because the chordwise and spanwise integrations are treated differently, they are discussed separately in the next two sections, the chordwise integration being discussed first.

TREATMENT OF THE INTEGRATION IN THE CHORDWISE DIRECTION

For the purpose of performing the chordwise integration it is convenient to replace the right side of the integral equation by a sum of separate integrals, each involving a particular chordwise pressure mode and in which the spanwise (η) and chordwise (ξ) integrations are separated. For this purpose equation (11) may be written as

$$\frac{w(x,y)}{V}=\frac{1}{8\pi q}\frac{4\rho V^2}{b}\sum_{m=0}^{\infty}\Big[a_{0m}\int_{span}g_m(\eta)I_0d\eta+\sum_{n=1}^{\infty}a_{nm}\int_{span}g_m(\eta)I_nd\eta\Big] \tag{13}$$

where

$$I_0=\int_{chord}f_0(\xi)K\Big[M,\frac{\omega}{V}(x-\xi),\frac{\omega}{V}(y-\eta)\Big]d\xi \tag{14a}$$

and

$$I_n=\int_{chord}f_n(\xi)K\Big[M,\frac{\omega}{V}(x-\xi),\frac{\omega}{V}(y-\eta)\Big]d\xi \tag{14b}$$

Remarks on methods of performing the chordwise integrations.—One could at this point evaluate the integrands of I_0 and I_n at small intervals of ξ and integrate by numerical means. This procedure would be difficult and tedious, however, since the kernel contains singularities and involves a large number of parameters and since the integrations would have to be carried out for many values of η. It is desirable to seek a simpler, but more approximate, approach which would be less laborious.

In the present analysis, an approach developed by Falkner in reference 25 (and discussed more fully in ref. 33) for the steady case is used which greatly reduces the amount of labor. In essence it is assumed that in the integrals I_0 and I_n, the loading modes $f_0(\xi)=\cot\frac{\theta}{2}$ and $f_n(\xi)=\sin n\theta$ can be replaced by an arbitrary but small number of replacement loads which are chosen in order to satisfy some integrated properties of the continuous loading. The use of this assumption will result in the integrals I_0 and I_n appearing finally as summations in the forms given by equations (20a) and (20b).

The use of a set of individual loads in performing the chordwise integrations and the procedures for evaluating them introduce approximations which are somewhat arbitrary. These approximations and their implications will be discussed later as they arise. They correspond to the assumptions made by Falkner and have been used in the present investigation for practical reasons. With high-speed computing equipment available, some of the approximations in the development which follows might be avoided. It can be stated, however, that, in the cases considered, the end results seem to be satisfactory.

Calculation of the replacement loads.—In calculating the values of the replacement loads, it is first required that the sum of the individual loads associated with a particular chordwise pressure mode must equal the integrated value of the continuous chordwise loading. If the continuous distribution is replaced by j replacement loads and $G_{\nu 0}$ and $G_{\nu n}$ denote loads associated, respectively, with the modes $\cot\theta/2$ and $\sin n\theta$, this equivalent load condition leads to the following set of equations:

$$\sum_{\nu=1}^{j} G_{\nu 0}=\int_0^{\pi}\cot\frac{\theta}{2}\sin\theta\,d\theta=\pi \tag{15a}$$

and

$$\left.\begin{aligned}\sum_{\nu=1}^{j} G_{\nu n}&=\int_0^{\pi}\sin n\theta\sin\theta\,d\xi=\frac{\pi}{2} \qquad (n=1)\\ \sum_{\nu=1}^{j} G_{\nu n}&=\int_0^{\pi}\sin n\theta\sin\theta\,d\xi=0 \qquad (n>1)\end{aligned}\right\} \tag{15b}$$

The use of equations (15) imposes one condition on the replacement loads G. However, equations (15) contain j unknowns; therefore, at least $j-1$ additional equations in terms of G are needed. In the present method the additional equations are obtained by requiring the downwash produced at selected points on the chord by the individual loads to equal the downwash due to the continuous load distribution. In imposing this condition the two-dimensional kernel function $\overline{K}$ is used instead of the more complicated three-dimensional downwash factor defined by equation (2). The relation between the two- and three-dimensional kernel functions is given by the following equation:

$$\overline{K}\left[M,\frac{\omega}{V}(x-\xi)\right]=\int_{-\infty}^{\infty}K\left[M,\frac{\omega}{V}(x-\xi),\frac{\omega}{V}(y-\eta)\right]d\eta$$

where $\overline{K}\left[M,\frac{\omega}{V}(x-\xi)\right]$ is the two-dimensional kernel.

The use of the two-dimensional downwash factor at this point is an intermediate step used only for evaluating G. In satisfying the actual downwash on the wing in the next section the calculated replacement loads are used with the three-dimensional kernel function. This intermediate use of the two-dimensional downwash factor implies that the areas close to a point contribute the major portion of the downwash at the point.

The $j-1$ additional equations in terms of G can be written by selecting $j-1$ positions, or control points, on the wing chord denoted by x_g at which to equate the downwash produced by the individual loads to that produced by the continuous loading. Although the lift conditions (eqs. (15)) did not require any assumption regarding the location of the replacement loads, for the purpose of employing the downwash condition such an assumption is necessary. In selecting this location an interpretation of the meaning of the replacement loads G is somewhat arbitrary. The replacement loads G can be considered as loads distributed over a certain portion of the wing chord, or they may be considered as concentrated loads operating at particular points on the chord. If the concept of a load distributed over an area is taken, then the distance to the downwash point is physically identifiable as some average distance, which for this particular case is measured from the center of the load area. If the concept of the concentrated load is used, then the distance is measured from the point of application of the load. In either case, a reference point x_ν is selected as the point of application of the load G so that the distance to the downwash point becomes x_g-x_ν. This distance is then used in developing the $j-1$ downwash equations for the determination of G.

For the $\cot\theta/2$ term of the loading series, the downwash equations are

$$\sum_{\nu=1}^{j} G_{\nu 0}\overline{K}_{g\nu}=\int_0^{\pi}\cot\frac{\theta}{2}\sin\theta\,\overline{K}_{g\xi}\,d\theta \tag{16a}$$

and, for the loading $\sin n\theta$, the downwash equations become

$$\sum_{\nu=1}^{j} G_{\nu n}\overline{K}_{g\nu}=\int_0^{\pi}\sin n\theta\sin\theta\,\overline{K}_{g\xi}\,d\theta \tag{16b}$$

where one such equation is obtained for each control-point location x_g selected. The functions $\overline{K}_{g\nu}$ and $\overline{K}_{g\xi}$ in equations (16) are defined as follows:

$$\overline{K}_{g\nu}=\overline{K}(M,Z_\nu)$$

and

$$\overline{K}_{g\xi}=\overline{K}(M,Z_\xi)$$

and represent the two-dimensional downwash factor tabulated by Schwarz (ref. 34). In these functions $Z_r=k(x_g-x_r)$ and $Z_\xi=k(x_g-\xi)$ where $k=\frac{b\omega}{V}$ and where a semichord b has been chosen for convenience as a reference length.

It should be noted that the integrands in equations (16a) and (16b) become infinite at $\xi=x$ and the integrals must be carefully treated. The method of handling these integrals is given in appendix B.

Other conditions which would not bring in consideration of the two-dimensional kernel could presumably be used for determining values of G. For example, in place of using the downwash conditions, $j-1$ additional equations could be written for each chordwise term of the loading series in which the first and higher (through $j-1$) moments of each load G could be equated to the corresponding moments produced by the continuous loading. By such a process, however, the loads G would not be a function of either frequency of oscillation or of Mach number. Through the use of the downwash conditions, some effects of both frequency and Mach number are included at this intermediate stage.

Illustrative equations for the loading functions.—In applying the method of this report, three chordwise pressure modes have been retained. The continuous distribution in each mode has been replaced by four individual replacement loads.

In order to evaluate the replacement loads, the lead established in the steady case with regard to locations of control points and loads has been followed. The loads are assumed to act at the ⅛-, ⅜-, ⅝-, and ⅞-chord positions, and the downwash conditions are applied at control points midway between the load stations, that is at the ¼-, ½-, and ¾-chord positions. Replacement loads based on these chordwise positions have been calculated for $M=0$, 0.5, and 1.0 and are presented in table I.

One set of replacement loads must be determined for each chordwise pressure mode. For the mode involving $\cot\theta/2$, the values of G_{rn} are determined from the following equations:

$$\left.\begin{aligned}
&G_{10}+G_{20}+G_{30}+G_{40}=\int_0^\pi \cot\frac{\theta}{2}\sin\theta\,d\theta=\pi\\
&G_{10}\overline{K}_{11}+G_{20}\overline{K}_{12}+G_{30}\overline{K}_{13}+G_{40}\overline{K}_{14}=\int_0^\pi \cot\frac{\theta}{2}\sin\theta\,\overline{K}_{1\xi}\,d\theta\\
&G_{10}\overline{K}_{21}+G_{20}\overline{K}_{22}+G_{30}\overline{K}_{23}+G_{40}\overline{K}_{24}=\int_0^\pi \cot\frac{\theta}{2}\sin\theta\,\overline{K}_{2\xi}\,d\theta\\
&G_{10}\overline{K}_{31}+G_{20}\overline{K}_{32}+G_{30}\overline{K}_{33}+G_{40}\overline{K}_{34}=\int_0^\pi \cot\frac{\theta}{2}\sin\theta\,\overline{K}_{3\xi}\,d\theta
\end{aligned}\right\}\quad(17)$$

where the functions $\overline{K}$ used here and in equations (18) and (19) are defined after equation (16b).

The first of these equations imposes the lift conditions stated by equation (15a). The remaining equations apply the downwash condition of equation (16a) at each of three control points; the second equation, for example, states that at control point 1 (at $x_g=x_1$ in eq. (16a)) the downwash produced by the four loads at $x_{r=1}$, $x_{r=2}$, $x_{r=3}$, and $x_{r=4}$ must equal the downwash produced at control point 1 by the continuous $\cot\theta/2$ loading.

A similar set of equations can be written for each chordwise pressure mode by using equations (15b) and (16b). For $\sin\theta$ the set of equations is

$$\left.\begin{aligned}
&G_{11}+G_{21}+G_{31}+G_{41}=\int_0^\pi \sin^2\theta\,d\theta=\frac{\pi}{2}\\
&G_{11}\overline{K}_{11}+G_{21}\overline{K}_{12}+G_{31}\overline{K}_{13}+G_{41}\overline{K}_{14}=\int_0^\pi \sin^2\theta\,\overline{K}_{1\xi}\,d\theta\\
&G_{11}\overline{K}_{21}+G_{21}\overline{K}_{22}+G_{31}\overline{K}_{23}+G_{41}\overline{K}_{24}=\int_0^\pi \sin^2\theta\,\overline{K}_{2\xi}\,d\theta\\
&G_{11}\overline{K}_{31}+G_{21}\overline{K}_{32}+G_{31}\overline{K}_{33}+G_{41}\overline{K}_{34}=\int_0^\pi \sin^2\theta\,\overline{K}_{3\xi}\,d\theta
\end{aligned}\right\}\quad(18)$$

and for $\sin 2\theta$,

$$\left.\begin{aligned}
&G_{12}+G_{22}+G_{32}+G_{42}=\int_0^\pi \sin\theta\sin 2\theta\,d\theta=0\\
&G_{12}\overline{K}_{11}+G_{22}\overline{K}_{12}+G_{32}\overline{K}_{13}+G_{42}\overline{K}_{14}=\int_0^\pi \sin\theta\sin 2\theta\,\overline{K}_{1\xi}\,d\theta\\
&G_{12}\overline{K}_{21}+G_{22}\overline{K}_{22}+G_{32}\overline{K}_{23}+G_{42}\overline{K}_{24}=\int_0^\pi \sin\theta\sin 2\theta\,\overline{K}_{2\xi}\,d\theta\\
&G_{12}\overline{K}_{31}+G_{22}\overline{K}_{32}+G_{32}\overline{K}_{33}+G_{42}\overline{K}_{34}=\int_0^\pi \sin\theta\sin 2\theta\,\overline{K}_{3\xi}\,d\theta
\end{aligned}\right\}\quad(19)$$

Use of the replacement loads G in the chordwise integration.—Once the replacement loads G have been determined, by solving equations (17), (18), and (19), continuous integrations indicated by equations (14) can be replaced by summations of the products of the loads G and the three-dimensional kernel function as follows:

$$I_0=b\sum_{r=1}^{j} G_{r0}K\left[M,\frac{\omega}{V}(x-x_r),\frac{\omega}{V}(y-\eta)\right]\qquad(20a)$$

and I_n (eq. 14b)) becomes

$$I_n=b\sum_{r=1}^{j} G_{rn}K\left[M,\frac{\omega}{V}(x-x_r),\frac{\omega}{V}(y-\eta)\right]\qquad(20b)$$

where the factor b arises through use of the substitution $\xi=-b\cos\theta$. In effect the continuous integrations have been represented by the replacement loads and a mean value of the kernel. These expressions may be substituted into equation (13) as follows:

$$\frac{w(x,y)}{V}=\frac{4\rho V^2}{8\pi q}\sum_{r=1}^{j}\sum_{n=0}^{\infty}\sum_{m=0}^{\infty}a_{nm}G_{rn}\int_{span}g_m(\eta)K\left[M,\frac{\omega}{V}(x-x_r),\frac{\omega}{V}(y-\eta)\right]d\eta\qquad(21)$$

leaving only the spanwise integration to be performed.

SPANWISE INTEGRATION

For the purpose of discussing the spanwise integration, equation (21) may be rewritten in simpler form as follows:

$$\frac{w(x,y)}{V}=\frac{1}{8\pi q}\sum_{r=1}^{j}\int_{span}\Delta P_r(\eta)K\left[M,\frac{\omega}{V}(x-x_r),\frac{\omega}{V}(y-\eta)\right]d\eta\qquad(22)$$

where

$$\Delta P_r(\eta)=4\rho V^2\sum_{n=0}^{\infty}\sum_{m=0}^{\infty}a_{nm}G_{rn}g_m(\eta)\qquad(23a)$$

or

$$\Delta P_\nu(\eta)=4\rho V^2\sqrt{s^2-\eta^2}\,[G_{\nu 0}(a_{00}+a_{01}\eta+a_{02}\eta^2)+G_{\nu 1}(a_{10}+a_{11}\eta+a_{12}\eta^2)+G_{\nu 2}(a_{20}+a_{21}\eta+a_{22}\eta^2+\ldots)+\ldots] \quad (23b)$$

Equation (23b) may be seen to correspond to the original form of the loading $\Delta p(\xi,\eta)$ given by equation (5a). In equations (23), however, the continuous chordwise-loading terms cot $\theta/2$ and sin $n\theta$ have been replaced by the loads $G_{\nu 0}$ and $G_{\nu n}$.

The integration of equation (22) may be handled by several procedures. A straightforward numerical integration could be performed for each value of x_ν by evaluating the kernel K at a number of spanwise stations. However, the kernel K contains some difficult singularities which have to be carefully considered. Moreover, in order to make tables of these integrals for general use, tables would have to be made for every aspect ratio, sweep angle, Mach number, and reduced frequency. In order to facilitate the development of tables, it is desirable to make use of a mean-value integration which involves integrating the kernel over a short segment of span and using the value of ΔP_ν at the midpoint of the segment. This method was followed in the present analysis and has the advantage that the integrals have to be tabulated only as functions of Mach number and reduced frequency.

The downwash at a point (x,y) due to a small element of span of length 2ϵ, the center of which is located at $\xi=x_\nu$ and $\eta=y_N$, is

$$\frac{\Delta w(x,y)}{V}=\frac{1}{8\pi q}\Delta P_\nu(y_N)\overline{F}_{\nu N} \quad (24)$$

where

$$\overline{F}_{\nu N}=\int_{y_N-\epsilon}^{y_N+\epsilon}K\left[M,\frac{\omega}{V}(x-x_\nu),\frac{\omega}{V}(y-\eta)\right]d\eta \quad (25a)$$

and where $\Delta P_\nu\,(y_N)$ refers to the value of ΔP_ν at the midpoint of the span element over which the integration extends.

The integral given by equation (25a) is of central importance in the present method and represents a "downwash factor" giving the downwash at a point (x,y) due to a unit pressure loading acting over a span element of length 2ϵ. The value of the integral depends only on the relative distance of the element from the point (x,y) and not on the spanwise location of the element on the wing. For convenience of calculation, therefore, it is desirable to perform a coordinate transformation to the center of the element, so that the integral appears as a function of distances from the point (x,y).

In order to perform this transformation, let $\eta'=\eta-y_N$ in equation (25a) where η' is a new spanwise variable. Equation (25a) can then be written as

$$\overline{F}_{\nu N}=\int_{-\epsilon}^{\epsilon}K\left[M,\frac{\omega}{V}(x-x_\nu),\frac{\omega}{V}(y-y_N-\eta')\right]d\eta'$$
$$=\int_{-\epsilon}^{\epsilon}K\left[M,\frac{\omega}{V}(x-x_\nu),\frac{\omega}{V}(y'-\eta')\right]d\eta' \quad (25b)$$

where $y'=y-y_N$ and where y' and η' are shown in sketch 2.

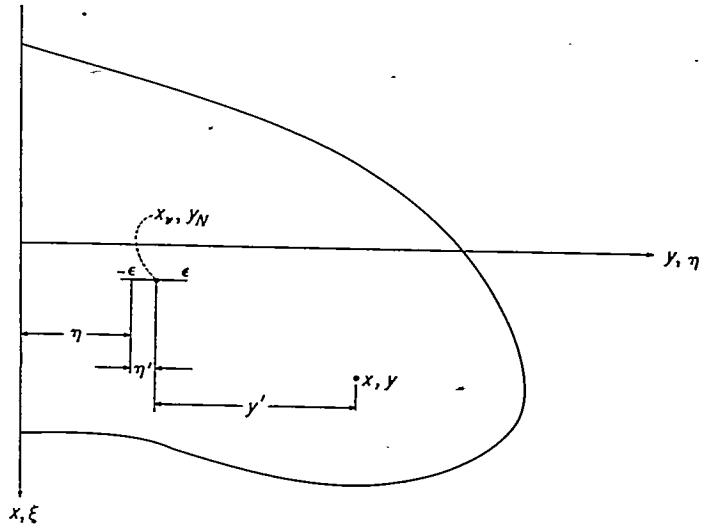

Sketch 2.

SELECTION OF REFERENCE LENGTHS

It is convenient at this point to choose certain reference lengths in both the downwash factor $\overline{F}_{\nu N}$, defined by equation (25b), and in the loading $\Delta P_\nu(y_N)$, defined by equations (23). In the case of the loading, the wing semispan s is chosen as a convenient reference length. If a new variable $\mu=y_N/s$ is introduced, the loading $\Delta P_\nu(y_N)$ can be written as

$$\Delta P_\nu(\mu)=4s\rho V^2\sum_{n=0}^{\infty}\sum_{m=0}^{\infty}a_{nm}g_m(\mu)G_{\nu n} \quad (26)$$

where

$$g_m(\mu)=\mu^m\sqrt{1-\mu^2}$$

and where μ is measured to the midpoint of the spanwise segment.

In the case of the downwash factor $\overline{F}_{\nu N}$, the length ϵ is taken as a reference length. The variables x, x_ν, y', and η' are then considered in a new sense to mean nondimensional quantities obtained by dividing the dimensional distances by the length ϵ. The downwash factor $\overline{F}_{\nu N}$ then appears as

$$\overline{F}_{\nu N}=\epsilon\int_{-1}^{1}K[M,\bar{k}(x-x_\nu),\bar{k}(y'-\eta')]\,d\eta'$$

where

$$\bar{k}=\frac{\epsilon\omega}{V}$$

The use of ϵ as a reference distance introduces a factor $1/\epsilon^2$ in the kernel (eq. (2)) as follows:

$$K[M,\bar{k}(x-\xi),\bar{k}(y-\eta)]=\frac{1}{\epsilon^2}\left\{\lim_{z\to 0}\frac{\partial^2}{\partial z^2}e^{-i\bar{k}(x-\xi)}\int_{-\infty}^{x-\xi}\frac{e^{\frac{i\bar{k}}{\beta^2}[\lambda-M\sqrt{\lambda^2+\beta^2(y-\eta)^2+\beta^2z^2}]}}{\sqrt{\lambda^2+\beta^2(y-\eta)^2+\beta^2z^2}}d\lambda\right\} \quad (27)$$

Equation (27) can be used to define a nondimensional kernel function $\underline{K}$ by writing

$$K[M,\bar{k}(x-x_\nu),\bar{k}(y'-\eta')]=\frac{1}{\epsilon^2}\underline{K}[M,\bar{k}(x-x_\nu),\bar{k}(y'-\eta')] \quad (28)$$

so that $\underline{K}$ in equation (28) corresponds to the quantity in braces in equation (27).

With the use of equation (28), the downwash factor $\overline{F}_{\nu N}$ appears as

$$\overline{F}_{\nu N}=\frac{1}{\epsilon}\int_{-1}^{1}\underline{K}\,[M,\bar{k}(x-x_\nu),\bar{k}(y'-\eta')]\,d\eta'$$

Finally, a nondimensional downwash factor $F_{\nu N}$ can be defined as

$$F_{\nu N}=\epsilon\overline{F}_{\nu N}=\int_{-1}^{1}\underline{K}\,[M,\bar{k}(x-x_\nu),\bar{k}(y'-\eta')]\,d\eta' \tag{29}$$

FINAL EXPRESSION FOR THE INTEGRAL EQUATION

Equations (26) and (29) can now be substituted into equation (24) to write a final expression for calculating the downwash at a point (x,y) on the wing. If the downwash due to all the span elements over the wing is summed, the total downwash becomes

$$\frac{w(x,y)}{V}=\frac{1}{8\pi q\epsilon}\sum_{\nu=1}^{j}\sum_{y_N}\Delta P_\nu(\mu)F_{\nu N} \tag{30a}$$

By using the expanded form for $\Delta P_\nu(\mu)$ given by equation (26), the total downwash can be written as (for $\epsilon=s/20$)

$$\frac{w(x,y)}{V}=\frac{40}{2\pi}\sum_{n}\sum_{m}\sum_{\nu}\sum_{y_N}a_{nm}G_{\nu n}g_m(\mu)F_{\nu N} \tag{30b}$$

The only unknowns in this equation are the coefficients a_{nm}. By selecting a number of control-point locations (x,y) at least equal to the number of a_{nm}'s desired, equation (30b) can be written for each control point. Thus, a set of simultaneous equations is obtained in terms of the coefficients a_{nm} which can then be calculated.

The next section is concerned with the calculation of the downwash factors $F_{\nu N}$ which have been defined in equation (29).

DETERMINATION OF DOWNWASH FACTOR F

The value of the downwash factor F (eq. (29)) for the oscillatory, compressible case is not available in the literature and consequently must be derived. However, the kernel K has been discussed in detail in reference 24, in which several forms of K are given. One form, as given by equation (20) of reference 24, would require a numerical integration in order to obtain F, since K cannot be integrated in closed form. Another form of the kernel, an expansion in terms of the frequency parameter $\bar{k}$, is given by equation (54) of reference 24 and is the form employed in the present analysis. In reference 24, a discussion is given of the accuracy of the frequency expansion. It is indicated that for moderate values of $\bar{k}$ and M the series is quite good for small distances $x-x_\nu$ and $y'-\eta'$. As $\bar{k}$ and the distances increase, the series deteriorates. Overall accuracy is not seriously affected, however, since the major contribution to the downwash at a point is from the nearby points on the surface.

Accordingly, the series is integrated term by term to obtain an approximate value for F. Several of the integrals are, however, improper, due to the existence of singularities in the integrand, and the concept of the principal value or finite part must be utilized. (See, for example, ref. 35 for a discussion of the finite part of integrals.) The results of the integration for an expansion to the 5th power of $\bar{k}$ is given in equation (31). (In presenting the expression for the downwash factor F, it is convenient to drop the primes on the quantities x' and y' and the bar on the reduced-frequency parameter $\bar{k}$. In the following expression, therefore, x, y, and k will be considered to denote the dimensionless quantities referred to ϵ unit length.)

$$\begin{aligned}
F_{\nu N}=&\int_{-1}^{1}\underline{K}(x_o,y-\eta)d\eta\\
=&e^{-ikx_o}\Bigg(\frac{x_o+R_1}{x_o(y+1)}-\frac{x_o+R_2}{x_o(y-1)}-\frac{ik}{\beta}\log\frac{\beta(y-1)+R_2}{\beta(y+1)+R_1}+\frac{k^2}{2\beta^2}\Bigg\{2\beta^2+2M-2\beta^2\log\frac{M+1}{\beta}+\frac{M^2x_o}{\beta}\log\frac{\beta(y-1)+R_2}{\beta(y+1)+R_1}-\\
&2\beta^2\left(\gamma-\frac{1}{2}+\frac{\pi i}{2}\right)+\beta^2(y+1)\left[\log\frac{x_o+R_1}{\beta(y+1)}-\log\frac{k(y+1)}{2}\right]-\beta^2(y-1)\left[\log\frac{x_o+R_2}{\beta(y-1)}-\log\frac{k(y-1)}{2}\right]\Bigg\}+\frac{ik^3}{6\beta^4}\Bigg\{4M^3x_o+\\
&\frac{3M^2x_o^2}{2\beta}\log\frac{\beta(y-1)+R_2}{\beta(y+1)+R_1}+\frac{3M^2-2}{2}\left[(y-1)R_2-(y+1)R_1\right]\Bigg\}+\frac{k^4}{96\beta^6}\Bigg\{-32M^3x_o^2-\frac{4}{3}M\beta^2(5M^2-3)(3y^2+1)-\\
&2\beta^6(y-1)^3\log\frac{x_o+R_2}{(M+1)(y-1)}+2\beta^6(y+1)^3\log\frac{x_o+R_1}{(M+1)(y+1)}-\frac{2M^2}{\beta}(M^2+4)x_o^3\log\frac{\beta(y-1)+R_2}{\beta(y+1)+R_1}+\\
&(2-4M^2-4M^4)x_o\left[(y-1)R_2-(y+1)R_1\right]+\beta^6\left[(y+1)^3-(y-1)^3\right]\left(-2\gamma+\frac{5}{2}+\frac{2}{3}-\pi i\right)+2\beta^6(y-1)^3\log\frac{k(y-1)}{2}-\\
&2\beta^6(y+1)^3\log\frac{k(y+1)}{2}\Bigg\}+\frac{ik^5}{360\beta^8}\Bigg\{-8M^3(5+M^2)x_o^3-\frac{15M^2}{8\beta}(3M^2+4)x_o^4\log\frac{\beta(y-1)+R_2}{\beta(y+1)+R_1}-8M^5\beta^2(3y^2+1)x_o-\\
&\frac{3\beta^2}{4}\left[(y-1)^3R_2-(y+1)^3R_1\right]+\frac{3}{8}(6-20M^2-15M^4)\left[(y-1)R_2-(y+1)R_1\right]x_o^2+\frac{5\beta^2}{4}(3M^2-1)\left[(y-1)R_2^3-\right.\\
&\left.(y+1)R_1^3\right]-16\beta^8y(y^2+1)+2\beta^8\left[(y+1)^4-(y-1)^4\right]\Bigg\}\Bigg)
\end{aligned} \tag{31}$$

where

$$R_1=\sqrt{x_o^2+\beta^2(y+1)^2} \qquad R_2=\sqrt{x_o^2+\beta^2(y-1)^2}$$

$$x_o=x-x_r \qquad \gamma=0.5772157$$

where $x_o=x-x_r$ is the distance from the line of integration to a control point, made nondimensional by dividing by ϵ, and is positive for locations of the control point behind the line of integration. The distance y is also nondimensionalized by ϵ and is positive to the right and is measured from the center of the integration segment as previously discussed. The reduced frequency k must also be based on the span segment ϵ and is accordingly

$$k=\frac{\epsilon\omega}{V}$$

Of course the number of spanwise segments N can be arbitrarily chosen. In general, the more segments taken the more accurate the result. Falkner (ref. 25) has used $\epsilon=s/20$ for most cases. As an example, the layout for a rectangular wing as used in the numerical example in appendix A is shown in figure 1.

The next section of the report is concerned with the application of the surface-loading method to the special case $M=1.0$.

THE SURFACE-LOADING METHOD FOR SONIC FLOW

The problem of calculating the forces for the limiting case of a wing which is oscillating in sonic flow is in general the same as for a wing at subsonic speeds with two exceptions. First, for the case of a sonic trailing edge, that is, when the trailing edge is perpendicular to the flow, the satisfaction of the Kutta condition ($\Delta p=0$ at trailing edge) is no longer necessary and another form of the series expansion for the loading Δp is applicable. (For the subsonic-trailing-edge case, i.e., when the trailing edge is not perpendicular to the flow, the loading series would, presumably, be of the same form as already shown for the subsonic case as given in eqs. (5).) The second difference between the sonic and subsonic cases lies in the form of the kernel K, which is used for the calculation of the downwash factor F as defined in equation (27). The modification of the kernel K to the limiting case $M=1$ has been performed in reference 24, but the integration

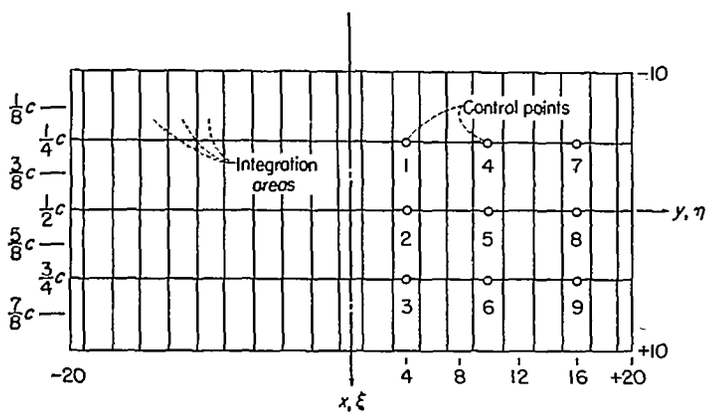

FIGURE 1.—Typical layout for lifting-surface method applied to a rectangular wing.

of the kernel with respect to the spanwise variable η must still be performed and is presented in another part of this section.

The present method is based on the usual assumptions of linearized theory and the use of this approximate theory may be open to question. However, for the very thin wings now being used on aircraft, it is felt that the first-order effects as given by linear theory constitute the major effects for unseparated flow and adequate solutions will be obtained.[2]

For the case of a sonic trailing edge the form selected for the loading is

$$\frac{\Delta p}{q}=\frac{8}{b}\sqrt{s^2-\eta^2}\left[\frac{1}{\sqrt{\xi-f_{le}}}(a_{00}+a_{01}\eta+a_{02}\eta^2+\ldots)+\sqrt{\xi-f_{le}}(a_{10}+a_{11}\eta+a_{12}\eta^2+\ldots)+(\xi-f_{le})^{3/2}(a_{20}+a_{21}\eta+a_{22}\eta^2+\ldots)+\ldots\right] \tag{32}$$

or

$$\frac{\Delta p}{q}=\frac{8}{b}\left[\sum_{n=0}^{\infty}\sum_{m=0}^{\infty}a_{nm}f_n(\xi-f_{le})g_m(\eta)\right] \tag{33}$$

where

$$f_n(\xi-f_{le})=(\xi-f_{le})^{n-\frac{1}{2}} \qquad (n=0,1,2,\ldots)$$

and

$$g_m(\eta)=\eta^m\sqrt{s^2-\eta^2}$$

This series contains some aspects of the supersonic case as well as the subsonic. For instance, as in the supersonic case, the loading is not zero at the trailing edge; whereas, as in the subsonic case, the loading becomes infinite at the leading edge.

TREATMENT OF INTEGRATION IN CHORDWISE DIRECTION

By following the scheme used for $M<1$, a set of simultaneous equations for the chordwise replacement loads is obtained corresponding to equations (15) and (16).

In calculating the values of the replacement loads, it is convenient to choose the semichord at some spanwise station as a reference length, as was done for $M<1$, and to perform a coordinate transformation such that the origin lies on the wing midline. By such a transformation a new chordwise loading function $f_n(\xi)$ can be defined as

$$f_n(\xi)=(1+\xi)^{n-\frac{1}{2}} \qquad (n=0,1,2,\ldots)$$

where ξ is now considered as a dimensionless variable based on a reference semichord and measured from the wing midline. In terms of this new variable ξ, the equations expressing the loading conditions (corresponding to eqs. (15) in the subsonic case) appear as

$$\sum_{\nu=1}^{J}G_{\nu n}=\int_{-1}^{1}(1+\xi)^{n-\frac{1}{2}}d\xi \tag{34}$$

[2] Some conditions which must be met in the linearization of the governing equations in the neighborhood of $M=1$ have been presented by Miles (ref. 36) and Mollo-Christensen (ref. 37). As stated by Miles, it is required that the conditions δ, $M\delta$, $K\delta$, $KM\delta<<1$ be satisfied and, in addition, that one or more of the following conditions be met:

$$|M-1|>>\delta^{1/3} \qquad k>>\delta^{1/3} \qquad \frac{1}{A}>>\delta^{1/3}$$

where δ is the thickness ratio, M is the Mach number, k is the reduced frequency, and A is the aspect ratio.

and for the downwash condition (corresponding to eqs. (16) in the subsonic case)

$$\sum_{r=1}^{j} G_{rn}\overline{K}_{gr}=\int_{-1}^{x_g}(1+\xi)^{n-\frac{1}{2}}\overline{K}_{g\xi}d\xi \tag{35}$$

where the functions $\overline{K}_{gr}$ and $\overline{K}_{g\xi}$ designate

$$\overline{K}_{gr}=\overline{K}[M,k(x_g-x_r)]_{M=1}$$

and

$$\overline{K}_{g\xi}=\overline{K}[M,k(x_g-\xi)]_{M=1}$$

and are the two-dimensional kernel as defined by equation (B23) of reference 24 and given in appendix B by equation (B9). Unlike the two-dimensional kernel for the subsonic case, these functions are not tabulated for $M=1$ and hence must be calculated.

In expanded form and for the nth chordwise-loading term, the set of simultaneous equations is

$$\left.\begin{aligned}
&G_{1n}+G_{2n}+G_{3n}+G_{4n}=\int_{-1}^{1}f_n(\xi)\,d\xi\\
&G_{1n}\overline{K}_{11}+G_{2n}\overline{K}_{12}+G_{3n}\overline{K}_{13}+G_{4n}\overline{K}_{14}=\int_{-1}^{x_1}f_n(\xi)\overline{K}_{1\xi}\,d\xi\\
&G_{1n}\overline{K}_{21}+G_{2n}\overline{K}_{22}+G_{3n}\overline{K}_{23}+G_{4n}\overline{K}_{24}=\int_{-1}^{x_2}f_n(\xi)\overline{K}_{2\xi}\,d\xi\\
&G_{1n}\overline{K}_{31}+G_{2n}\overline{K}_{32}+G_{3n}\overline{K}_{33}+G_{4n}\overline{K}_{34}=\int_{-1}^{x_3}f_n(\xi)\overline{K}_{3\xi}\,d\xi
\end{aligned}\right\} \tag{36}$$

A set of simultaneous equations as given by equation (36) must be formed for each value of n and solved for the associated values of G.

As in the case of subsonic flow, the integrands of the integrals of equation (36) become infinite at $\xi=x_g$. The evaluation of these integrals is discussed in the latter part of appendix B.

At sonic conditions, a disturbance cannot be propagated upstream, so that the labor of computing the loading functions is reduced as compared with the case for $M<1$ since the downwash factors do not have to be determined and summed for conditions where the control point is upstream of the integration area.

As an example, if the loading functions are assumed to act at the ⅛-, ⅜-, ⅝-, and ⅞-chord positions and the control points are located at the ¼-, ½-, and ¾-chord positions, then

$$K_{12}=K_{13}=K_{14}=K_{23}=K_{24}=K_{34}=0$$

since the terms represent downwash factors for control points ahead of the loading stations. Thus, the set of equations becomes triangular and can be solved by successive substitutions.

TREATMENT IN SPANWISE DIRECTION

The integration in the span direction is carried out in the same manner as was done for $M<1$, that is, the wing is divided into many small segments, and, with the load Δp assumed to be constant across the segment, the integration is performed. The kernel for this case is given by equations (47) in reference 24. However, it is not possible to integrate this expression for the kernel in closed form and, as was done for the case when $M<1$, the kernel was expanded in powers of the frequency parameter k and integrated term by term. The concept of the principal part of a finite integral was used. The form of the integrated series is given in the following equation:

$$\begin{aligned}
F_{M=1}&=\int_{-1}^{1}\underline{K}[M,kx_o,k(y'-\eta')]_{M=1}\,d\eta'\\
&=2e^{-\frac{ikx_o}{2}}\left\{\frac{1}{y+1}-\frac{1}{y-1}+\frac{ik}{x_o}+\frac{k^2}{24x_o^2}[(y+1)^3-(y-1)^3]-\frac{ik^3}{240x_o^3}[(y+1)^5-(y-1)^5]-\frac{k^4}{2{,}688x_o^4}[(y+1)^7-(y-1)^7]+\right.\\
&\left.\frac{ik^5}{34{,}560x_o^5}[(y+1)^9-(y-1)^9]\right\}+e^{-ikx_o}\left(ikx_o\left(\frac{1}{y-1}-\frac{1}{y+1}\right)+\frac{k^2}{2}\left[2\left(1-\gamma-\frac{\pi i}{2}+\log\frac{2x_o}{k}\right)-\frac{x_o^2}{2}\left(\frac{1}{y-1}-\frac{1}{y+1}\right)-\right.\right.\\
&\left.(y+1)\log(y+1)^2+(y-1)\log(y-1)^2+2(y+1)-2(y-1)\right]+\frac{ik^3}{6}\left\{3x_o-\frac{x_o^3}{4}\left(\frac{1}{y-1}-\frac{1}{y+1}\right)+\frac{1}{4x_o}[(y+1)^3-(y-1)^3]\right\}+\\
&\frac{k^4}{96}\left\{(3-2\gamma-\pi i)[(y+1)^3-(y-1)^3]-6x_o^2+\frac{x_o^4}{2}\left(\frac{1}{y-1}-\frac{1}{y+1}\right)+\frac{(y+1)^5-(y-1)^5}{5x_o^2}+2[(y+1)^3-(y-1)^3]\log\frac{2x_o}{k}-\right.\\
&\left.2[(y+1)^3\log(y+1)^2-(y-1)^3\log(y-1)^2-\frac{2}{3}(y+1)^3+\frac{2}{3}(y-1)^3]\right\}+ik^5\left\{-\frac{2x_o^3}{288}+\frac{x_o}{192}[(y+1)^3-(y-1)^3]+\right.\\
&\left.\left.\frac{(y+1)^5-(y-1)^5}{480x_o}-\frac{(y+1)^7-(y-1)^7}{8{,}064x_o^3}+\frac{x_o^5}{1{,}920}\left(\frac{1}{y-1}-\frac{1}{y+1}\right)\right\}\right)
\end{aligned} \tag{37}$$

where the parameters x_o, y, k, and γ are identical to those employed in equation (31).

REMARKS PERTINENT TO THE SURFACE-LOADING METHOD

In previous sections of this report, some of the approximations involved in the present lifting-surface method have been discussed. It has been pointed out that certain arbitrary features arise in performing the numerical evaluations of the integrals, particularly with regard to the chordwise integrations. The assumptions that have been made in this connection include the replacement of the continuous chordwise loading by a number of individual replacement loads, the use of the two-dimensional kernel function in evaluating these loads, and the choice of a set of load stations at which the replacement loads are assumed to act. In addition, a set of control points must be selected at which the governing downwash conditions are to be satisfied. In the actual application of the procedure these features give rise to certain problems which are discussed in the following paragraphs.

CONTROL-POINT AND LOAD-STATION LOCATION

No attempt has been made in this report to determine the most favorable location of the control points or the optimum location for the stations at which the replacement loads are assumed to act. For such a study, systematic tables of the downwash factor are desirable and when these tables become available, it will be much easier to evaluate this aspect of the problem. In the present study, such tables were not available, and the positions of the control points and the means of distributing the loading selected were the same as have been used for the steady case. It is felt that, at least for the simple rigid modes considered in the present study, the location of the control points is not critical. For more complicated modes of deformation other locations and additional control points might be necessary. This question is worthy of further study.

EFFECT OF TAPER

In the calculation of the distribution of the loading across the chord, it is necessary to select a value of the reduced frequency $k=\frac{b\omega}{V}$ to be used in calculating the two-dimensional downwash factors $\overline{K}_{g\eta}$ and $\overline{K}_{g\xi}$ in the integrals in equations (16). For a tapered wing, the problem arises as to what span position to use to obtain a reference chord for calculating k.

In relation to this effect of taper, as a part of the present investigation, two separate calculations were made for the case of a 45° delta wing. In one case, the root chord was used as the reference chord, whereas, in the other, the chord at the midsemispan was used. It was found that the final results obtained for the pressure distribution and, consequently, for the lift and moment from the two calculations were almost identical. On the basis of this one test case, it may be inferred that the location of the reference chord is not an important factor. In the remainder of the delta-wing calculations presented in this report, the chord at midsemispan was used.

DISCUSSION OF SOME APPLICATIONS OF THE METHOD

This section is concerned with a discussion of the results of calculations which were based on the lifting-surface method discussed. Calculations have been made for both rectangular and triangular wings and comparisons of the results have been made with existing theoretical and experimental results where possible.

RECTANGULAR WING

In order to furnish a basis for comparison of results of the method with existing theory, calculations have been performed at $M=0$ for a rectangular wing with an aspect ratio of 2 pitching about the midchord for various values of the reduced frequency k. The results are compared with the results given by Lawrence and Gerber (ref. 29) and are shown plotted in figure 2. In figure 2 (a) the magnitudes are plotted, and in figure 2 (b) the corresponding phase angles are plotted. Excellent agreement is obtained for both the

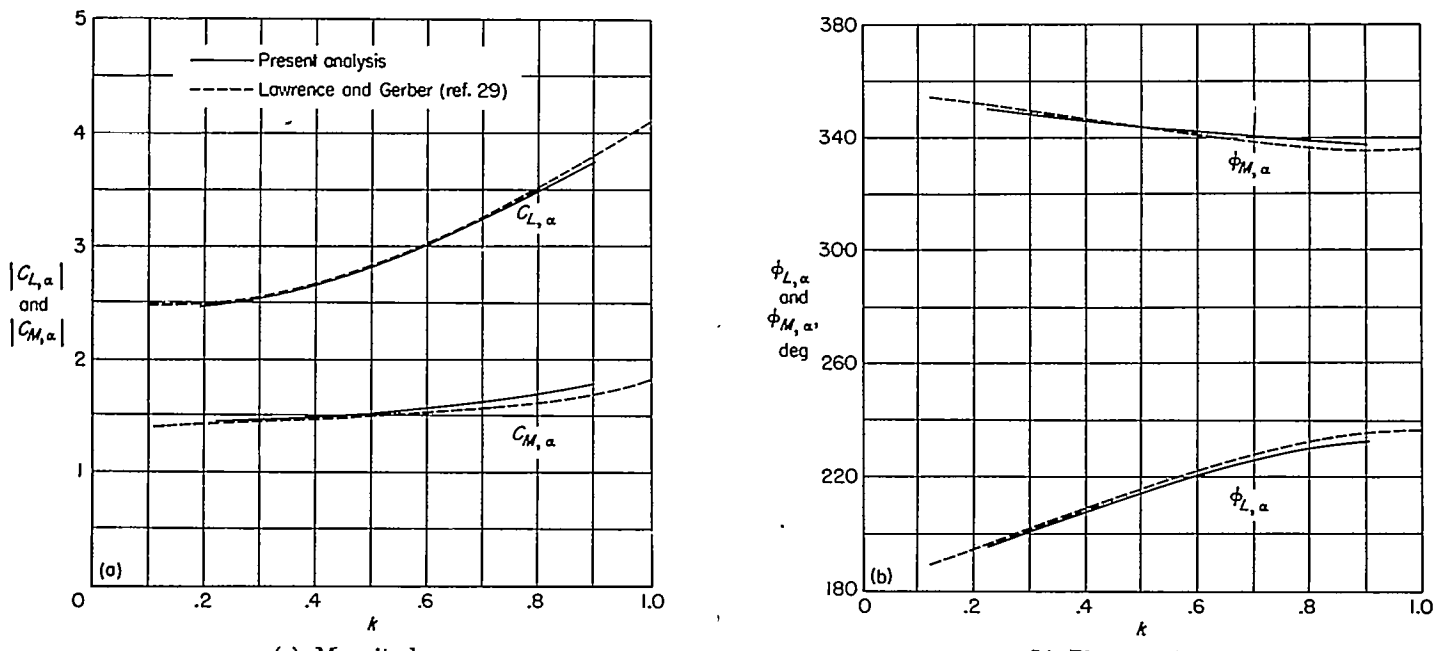

(a) Magnitude. (b) Phase angle.

FIGURE 2.—Variation of lift and moment with reduced frequency k for a rectangular wing oscillating in pitch about its midchord. $A=2$; $M=0$.

magnitude and the phase angle. Although both the present method and the method of Lawrence and Gerber are approximate, the good agreement between the results promotes a feeling of confidence in both methods. It should be noted that the two methods are not similar and contain entirely different approximations.

To obtain some effects of Mach number, calculations were made for the same rectangular wing with aspect ratio of 2 pitching about the midchord for a range of Mach numbers at a constant value of $k=0.22$. Results are shown in figure 3. Included in the figure are the results of two-dimensional calculations. The magnitudes of the lift and moment are given in figure 3 (a) and the corresponding phase angles are given in figure 3 (b). Calculations for three-dimensional flow up to and including $M=1$ were made by the use of the surface-loading method. The results at supersonic speeds were obtained from reference 12. The variation with Mach number for both the lift and moment is approximately that which would be predicted by use of the factor $\sqrt[4]{1-M^2}$ up to $M=0.7$. Both the moment and lift increase at $M=1$ and then drop off again at supersonic speed. Note that the two-dimensional lift coefficient has the same shape for the range up to $M=0.7$ and that application of the aspect-ratio correction factor $\frac{A}{A+2}=\frac{1}{2}$ would apply fairly well. No such simple factor exists for the phase angles, and it would not be possible to correct two-dimensional results for finite span effects.

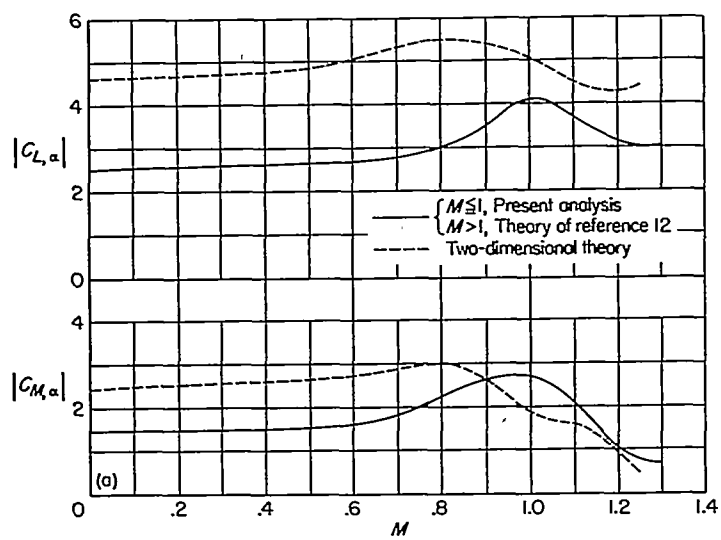

(a) Magnitude.

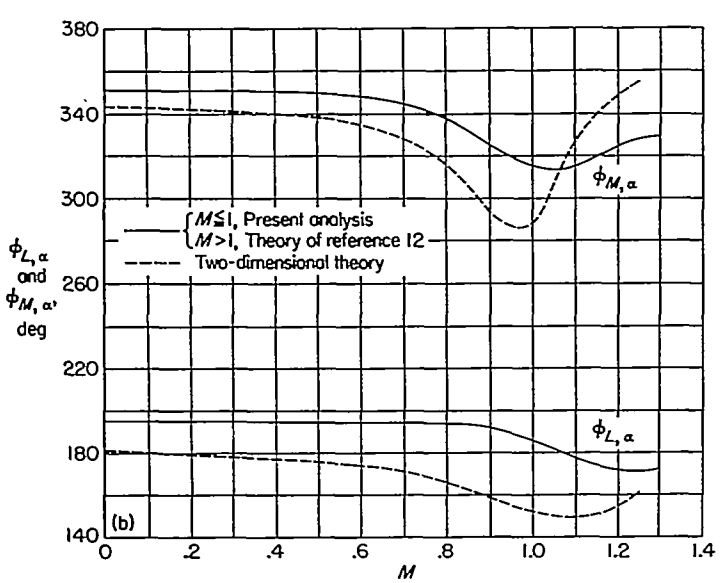

(b) Phase angle.

FIGURE 3.—Variation of lift and moment with Mach number for a rectangular wing oscillating in pitch about its midchord. $A=2$; $k=0.22$.

TRIANGULAR WING

Figures 4 and 5 present results for a delta wing with an aspect ratio of 4 oscillating in pitch about the midchord. In figure 4 is shown the lift and associated phase angles plotted against the reduced frequency k for $M=0$. Results of the present analysis as shown by the solid line and those of Lawrence and Gerber (ref. 29) as shown by the dashed line are compared with some experimental results (indicated by the circles) obtained by Sumner A. Leadbetter and Sherman A. Clevenson at the Langley Aeronautical Laboratory. It is noteworthy that the results of the two methods agree rather well, even with respect to phase angle.

In figure 5 a corresponding comparison for the moment and its associated phase angle (for the same wing and for the same conditions as in fig. 4) is shown plotted against the reduced frequency k. Results of both analyses are in substantial agreement with respect to the magnitude of the moment. With regard to the phase angles, a significant difference between the results of the two theories occurs, although both theories indicate the same trend. The source of the difference can not be explained at the present time and will have to be resolved by further calculations and experiments.

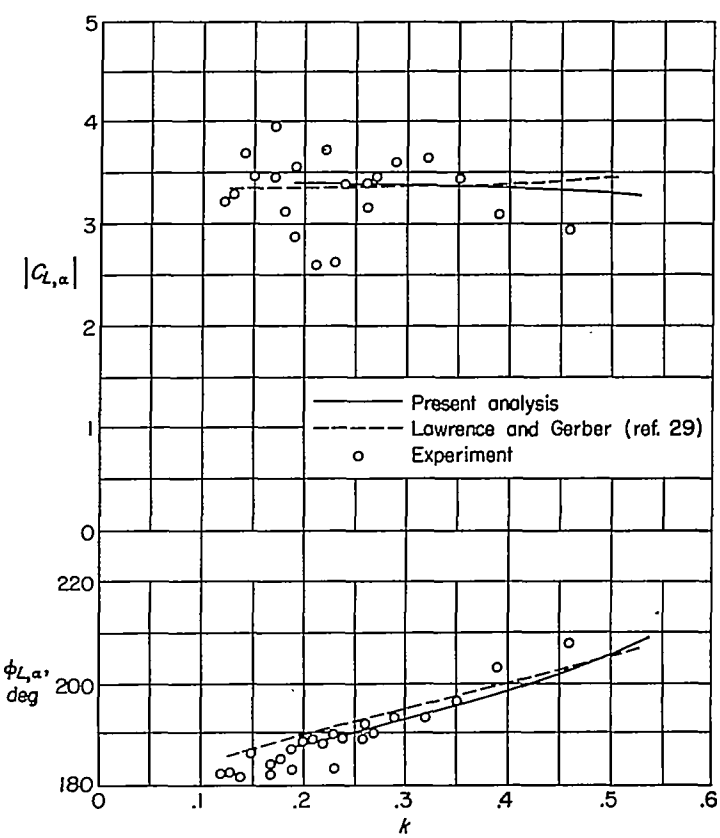

FIGURE 4.—Variation of lift with reduced frequency k for a delta wing oscillating in pitch about its midchord. $A=4$; $M=0$.

RESULTS OF MULTIPLE-LINE METHOD

Figure 6 shows results of calculations for a rectangular wing with an aspect ratio of 2 at $M=0$ based on the multiple-line method described in appendix D. Results of the line method approach those of the surface-loading method when a fairly large number of lifting lines and control points are used. These results are discussed more fully in appendix D.

CONCLUDING REMARKS

The purpose of this report has been to present and describe in detail a method for calculating the loading on a wing of any practical plan form which is oscillating in a subsonic or sonic stream. The method is presented in general form and some results of application are discussed. A sample calculation for a specific case is presented in an appendix. The method may be used for calculating the loading on elastic wings as well as on rigid wings. This feature makes the method adaptable to flutter calculations since it is possible to calculate the loading for the various modes usually assumed for a normal type of modal flutter analysis. The method can also be applied in principle, at least, to the combined aerodynamic and structural problem in which the flutter characteristics are obtained directly by the use of structural and aerodynamic influence coefficients.

The procedure used is based on linearized theory in which the usual assumptions of linearized flow, such as small thickness ratio of the wing, inviscid fluid, and so forth, are necessary.

The method has been found to give good agreement with existing theory and experiment for low subsonic Mach numbers for both rectangular and triangular wings. Results for high subsonic Mach numbers and a Mach number of 1 fit in well with theoretical results for supersonic flow but require further verification by comparison with experiment.

In addition to the presentation of the lifting-surface method, a multiple-line approach is included in an appendix. Results of the line method approach those of the surface-loading method when a fairly large number of lifting lines and control points are used.

It is realized that several variants of the procedure may be made and may be desirable for routine or systematic calculations, particularly in view of the constantly increasing capabilities of automatic computing equipment.

LANGLEY AERONAUTICAL LABORATORY,
NATIONAL ADVISORY COMMITTEE FOR AERONAUTICS,
LANGLEY FIELD, VA., *March 14, 1956.*

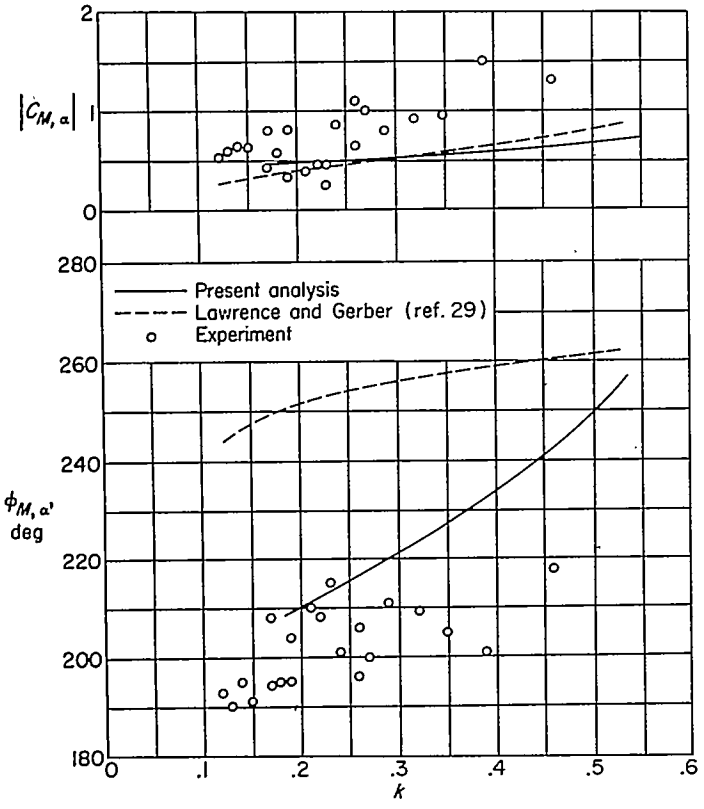

FIGURE 5.—Variation of moment with reduced frequency k for a delta wing oscillating in pitch about its midchord. $A=4$; $M=0$.

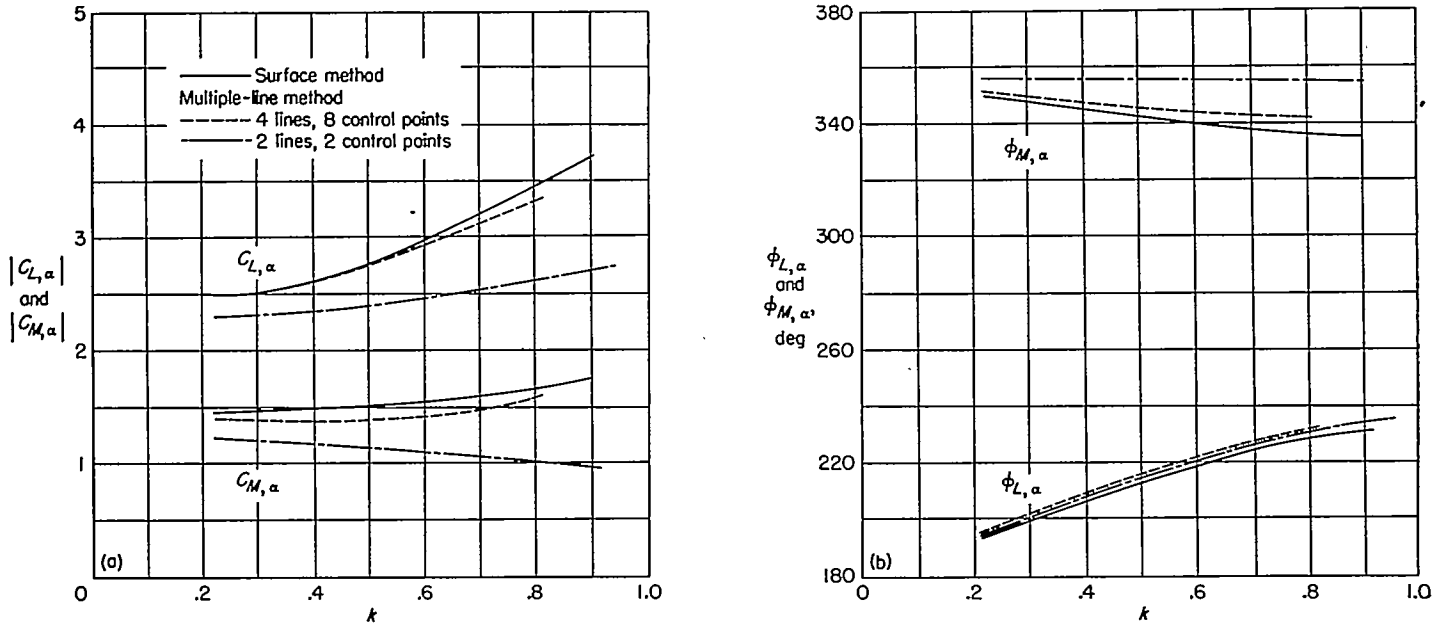

(a) Magnitude. (b) Phase angle.

FIGURE 6.—Variation of lift and moment with reduced frequency k for a rectangular wing oscillating in pitch about its midchord. Comparison of results of multiple-line method with results of surface-loading method. $A=2$; $M=0$.

APPENDIX A

NUMERICAL EXAMPLE OF THE LIFTING-SURFACE METHOD FOR A RECTANGULAR WING

$(A=2;\ k=0.22;\ M=0.5)$

As an illustration of the calculation procedure of the lifting-surface method, the details of the procedure are presented in this appendix for a rectangular wing with $A=2$ and $k=0.22$, which is oscillating as a rigid wing about the midchord line in a stream flow of $M=0.5$. For the case of subsonic flow the main equation to be dealt with is equation (30a) or (30b). The steps in performing the calculations are as follows:

(1) The first step in the process is to divide the wing into a number of areas as shown in figure 1, to select the number and location of the control points, and, consequently, to determine the number of terms of the loading series (eqs. (5)) which are to be retained. For the present case, the wing was divided into four equal chordwise areas for the calculation of the distribution of the load in the chord direction. For the spanwise integration, the wing was divided into 21 segments of which 19 are segments of span 2ϵ and two (one at each tip) are of span ϵ. The semispan ϵ of a segment is thus equal to one-twentieth the wing semispan. (In all of the calculations this quantity ϵ is used as a nondimensionalizing factor so that the full wing span becomes 40 units. For a wing with $A=2$, as considered in this example, the chord is therefore 20 units and extends from -10 at the leading edge to 10 at the trailing edge. The reduced-frequency parameter k (based on the half-chord) in terms of ϵ becomes $\bar{k}=\frac{k\epsilon}{b}=\frac{\epsilon\omega}{V}$ and for this example $k=0.22$ and $\bar{k}=0.022$.)

Nine control points located at the ¼-, ½-, and ¾-chord positions and at three span stations $\eta=0.2$, 0.5, and 0.8 of the wing semispan were selected. The selection of nine control points determines the minimum number of terms of the loading series. There can be more control points than terms of the loading series; however, a method of least squares would have to be employed for the final solution.

In the present example, nine terms were retained in the loading series. Three chordwise terms, each modified by three spanwise terms, were used so that the series contains nine unknown coefficients a_{nm} and appears as

$$\frac{\Delta p}{q}=\frac{8}{b}\sqrt{s^2-\eta^2}\left[\cot\frac{\theta}{2}(a_{00}+a_{02}\eta^2+a_{04}\eta^4)+\sin\theta(a_{10}+a_{12}\eta^2+a_{14}\eta^4)+\sin 2\theta(a_{20}+a_{22}\eta^2+a_{24}\eta^4)\right] \tag{A1}$$

It is only necessary to consider the even power terms in η since the loading is assumed to be symmetrical in the span direction about the midspan position.

(2) The next step consists of calculating the replacement loads G from equations (17), (18), and (19). For the present case, there are three ($n=0$, 1, or 2) sets of four simultaneous equations as follows:

$$\left.\begin{aligned}
&G_{1n}+G_{2n}+G_{3n}+G_{4n}=\int f_n(\xi)\,d\xi\\
&(-2.83500-0.45000i)G_{1n}+(2.25500-0.47680i)G_{2n}+(0.60680-0.29670i)G_{3n}+(0.29180-0.22086i)G_{4n}=\int f_n(\xi)\overline{K}_{1\xi}\,d\xi\\
&(-1.17430-0.21760i)G_{1n}+(-2.83500-0.45000i)G_{2n}+(2.25500-0.47680i)G_{3n}+(0.60680-0.29670i)G_{4n}=\int f_n(\xi)\overline{K}_{2\xi}\,d\xi\\
&(-0.85000-0.09037i)G_{1n}+(-1.17430-0.21760i)G_{2n}+(-2.83500-0.45000i)G_{3n}+(2.25500-0.47680i)G_{4n}=\int f_n(\xi)\overline{K}_{3\xi}\,d\xi
\end{aligned}\right\} \tag{A2}$$

The coefficients of the replacement loads G are values of the two-dimensional kernel $\overline{K}_{mn}$ and have been obtained directly from the table of reference 34. The kernel $\overline{K}_{mn}$ is a function of M, and $Z=\bar{k}(x-\xi)$. Consider as an example the center of area at ⅛ chord $\left(\xi=\frac{-30}{4}\right)$ and a control point at ¼ chord ($x=-5$). For $\bar{k}=0.022$, $Z=(0.022)\left(-5+\frac{30}{4}\right)=0.055$ and for $M=0.5$, the downwash factor $\overline{K}_{11}=-2.83500-0.45000i$ may be read from the table of reference 34. Similarly, for the same values of $\bar{k}$ and M and for the center of area at ⅞ chord $\left(\xi=\frac{30}{4}\right)$ and the control point at midchord ($x=0$), $Z=0.022\left(0-\frac{30}{4}\right)=-0.165$ and, therefore, $\overline{K}_{12}=0.60680-0.29670i$.

The integrals on the right of equation (A2) are given as follows for the three sets of equations corresponding to $n=0$, 1, and 2. (See appendix B for discussion of method of integration.)

For $n=0, f_0(\xi)=\cot\frac{\theta}{2}$ and

$$\left.\begin{aligned}
&\int_0^\pi \cot\frac{\theta}{2}\sin\theta\, d\theta=\pi\\
&\int_0^\pi \cot\frac{\theta}{2}\overline{K}_{1\xi}\sin\theta\, d\theta=-2.88354-1.34125i\\
&\int_0^\pi \cot\frac{\theta}{2}\overline{K}_{2\xi}\sin\theta\, d\theta=-2.97504-0.96137i\\
&\int_0^\pi \cot\frac{\theta}{2}\overline{K}_{3\xi}\sin\theta\, d\theta=-3.03074-0.57320i
\end{aligned}\right\}\quad\text{(A3)}$$

For $n=1, f_1(\xi)=\sin\theta$ and

$$\left.\begin{aligned}
&\int_0^\pi \sin^2\theta\, d\theta=\frac{\pi}{2}\\
&\int_0^\pi \sin^2\theta\,\overline{K}_{1\xi}\, d\theta=0.58912-0.63606i\\
&\int_0^\pi \sin^2\theta\,\overline{K}_{2\xi}\, d\theta=-0.45095-0.67032i\\
&\int_0^\pi \sin^2\theta\,\overline{K}_{3\xi}\, d\theta=-1.48547-0.55366i
\end{aligned}\right\}\quad\text{(A4)}$$

For $n=2, f_2(\xi)=\sin 2\theta$ and

$$\left.\begin{aligned}
&\int_0^\pi \sin 2\theta\sin\theta\, d\theta=0\\
&\int_0^\pi \sin 2\theta\sin\theta\,\overline{K}_{1\xi}\, d\theta=-1.03882-0.20631i\\
&\int_0^\pi \sin 2\theta\sin\theta\,\overline{K}_{2\xi}\, d\theta=-2.02994+0.04145i\\
&\int_0^\pi \sin 2\theta\sin\theta\,\overline{K}_{3\xi}\, d\theta=-1.02892+0.28861i
\end{aligned}\right\}\quad\text{(A5)}$$

The values of G as computed from the three sets of simultaneous equations formed by substituting equations (A3), (A4), and (A5) into equation (A2) are

$$\left.\begin{aligned}
&G_{10}=1.72184+0.00224i\\
&G_{20}=0.73737-0.01130i\\
&G_{30}=0.44052-0.00484i\\
&G_{40}=0.24186+0.01389i\\
&G_{11}=0.30752+0.02241i\\
&G_{21}=0.47670+0.00582i\\
&G_{31}=0.47702-0.00583i\\
&G_{41}=0.30956-0.02240i\\
&G_{12}=0.45744+0.01103i\\
&G_{22}=0.23804-0.01055i\\
&G_{33}=-0.23753-0.01073i\\
&G_{42}=-0.45795+0.01024i
\end{aligned}\right\}\quad\text{(A6)}$$

When the values of G are obtained, the loading function $\Delta P_\nu(\mu)$ appearing in equation (30a) and defined by equation (26) may be written as

$$\Delta P_\nu(\mu)=4s\pi\rho V^2\sqrt{1-\mu^2}\,[G_{\nu 0}(a_{00}+a_{02}\mu^2+a_{04}\mu^4)+ G_{\nu 1}(a_{10}+a_{12}\mu^2+a_{14}\mu^4)+G_{\nu 2}(a_{20}+a_{22}\mu^2+a_{24}\mu^4)]\quad\text{(A7)}$$

where $\nu=1$, 2, 3, or 4 corresponding to the 4 areas in the chord direction.

Examination of this equation shows that certain products of $G_{\nu n}\mu^m\sqrt{1-\mu^2}$ are needed. These products correspond to the products $g_m(\mu)G_{\nu n}$ in equation (30b). It has been found convenient to arrange these products in a certain form for later calculations. This form is shown in table II where values of the products are given for the complete system of replacement loads.

(3) The downwash factors F must now be determined. These factors may be calculated by the use of equation (31), which was used for this example. With the adaptation of high-speed computing machines to the problem, the kernel in the form of equation (20) of reference 24 may be numerically integrated without, perhaps, the frequency and Mach number restriction of the series. However done, the distance between the centers of areas and the control points, x_o and y', must first be determined. For the present case, the y' distances for control point 1 and the first chordwise area corresponding to $g=1$, for example, are

ρ	0	0.1	0.2	0.3	0.4	0.5	0.6	0.7	0.8	0.9
y'_R------	4	2	0	2	4	6	8	10	12	14
y'_L------	---	6	8	10	12	14	16	18	20	22

The distance $x=2.5$ is constant since the wing is rectangular.

Since the loading in the example is symmetrical about the midspan, the loading factors which multiply F in equation (30b) are the same for equidistance on each side of the midspan. Therefore, the values of F which are located at equal distances from the midspan may be computed and added before multiplication by the loading; consequently, distances y'_R and y'_L have been given in the example where y'_R refers to the distance from a control point to the centers of the areas to the right of the wing midspan and y'_L refers to distances to areas to the left of the midspan. The final form of the F factors is given in table III where, for each entry, the two values of F for y'_R and y'_L have been added.

(4) The next step is the multiplication of the loading factors of table II by the downwash factors F of table III in accordance with equation (30b) which results in a 9 by 9 matrix of complex elements. This is given by the left side of the following equation and the downwash conditions to be discussed subsequently are shown on the right of the equation:

$$\left.\begin{aligned}
&(1.07713+0.18156i)a_{00}+(-0.05279+0.09589i)a_{10}+(0.33112+0.04129i)a_{20}+(-0.14365+0.04387i)a_{02}+\\
&(-0.05511+0.01465i)a_{12}+(-0.02878+0.00716i)a_{22}+(-0.07449+0.01803i)a_{04}+(-0.02325+0.00588i)a_{14}+\\
&(-0.01569+0.00262i)a_{24}=-(0.025-0.00275i)2\pi\\[6pt]
&(1.20324+0.02339i)a_{00}+(0.27977+0.08613i)a_{10}+(0.60908-0.03442i)a_{20}+(-0.21994+0.06173i)a_{02}+\\
&(-0.08525+0.02208i)a_{12}+(-0.03123+0.00921i)a_{22}+(-0.10617+0.02758i)a_{04}+(-0.03939+0.00924i)a_{14}+\\
&(-0.01984+0.00434i)a_{24}=-(0.025+0i)2\pi\\[6pt]
&(1.28588-0.12323i)a_{00}+(0.60852+0.03132i)a_{10}+(0.32497-0.10481i)a_{20}+(-0.26574+0.08792i)a_{02}+\\
&(-0.11441+0.03304i)a_{12}+(-0.02668+0.01177i)a_{22}+(-0.12604+0.04013i)a_{04}+(-0.05509+0.01447i)a_{14}+\\
&(-0.01473+0.00615i)a_{24}=-(0.025+0.00275i)2\pi\\[6pt]
&(0.90622+0.11076i)a_{00}+(0.01456+0.06672i)a_{10}+(0.27334+0.02249i)a_{20}+(0.95139+0.00148i)a_{02}+\\
&(0.11217+0.02272i)a_{12}+(0.25999+0.00395i)a_{22}+(0.65180-0.00715i)a_{04}+(0.08428+0.01228i)a_{14}+\\
&(0.17638+0.00116i)a_{24}=-(0.025-0.00275i)2\pi\\[6pt]
&(1.11514-0.01962i)a_{00}+(0.29257+0.05294i)a_{10}+(0.47578-0.03410i)a_{20}+(1.24921-0.13010i)a_{02}+\\
&(0.37821-0.00132i)a_{12}+(0.41833-0.04271i)a_{22}+(0.86338-0.09666i)a_{04}+(0.26493-0.00490i)a_{14}+\\
&(0.28075-0.02977i)a_{24}=-(0.025+0i)2\pi\\[6pt]
&(1.23341-0.15624i)a_{00}+(0.56690+0.00126i)a_{10}+(0.26664-0.08806i)a_{20}+(1.42203-0.28189i)a_{02}+\\
&(0.63972-0.06063i)a_{12}+(0.25104-0.08838i)a_{22}+(0.98606-0.20164i)a_{04}+(0.44244-0.04595i)a_{14}+\\
&(0.17013-0.06028i)a_{24}=-(0.025+0.00275i)2\pi\\[6pt]
&(1.01349+0.15772i)a_{00}+(-0.03208+0.08573i)a_{10}+(0.30911+0.03520i)a_{20}+(0.25606+0.03542i)a_{02}+\\
&(-0.00455+0.01979i)a_{12}+(0.07656+0.00815i)a_{22}+(-0.04884+0.02325i)a_{04}+(-0.02859+0.00797i)a_{14}+\\
&(-0.00894+0.00448i)a_{24}=-(0.025-0.00275i)2\pi\\[6pt]
&(1.15764+0.00975i)a_{00}+(0.27905+0.07481i)a_{10}+(0.56079-0.03381i)a_{20}+(0.29204-0.00192i)a_{02}+\\
&(0.07234+0.01661i)a_{12}+(0.13788-0.00879i)a_{22}+(-0.09262+0.02861i)a_{04}+(-0.03866+0.01133i)a_{14}+\\
&(-0.00479+0.00393i)a_{24}=-(0.025+0i)2\pi\\[6pt]
&(1.24922-0.13126i)a_{00}+(0.58649+0.02187i)a_{10}+(0.30293-0.09826i)a_{20}+(0.31639-0.03720i)a_{02}+\\
&(0.14828+0.00321i)a_{12}+(0.07495-0.02452i)a_{22}+(-0.11594+0.04007i)a_{04}+(-0.04833+0.01603i)a_{14}+\\
&(-0.00800+0.00402i)a_{24}=-(0.025+0.00275i)2\pi
\end{aligned}\right\}\qquad\text{(A8)}$$

(5) The boundary conditions w at the various control points are determined from the motion of the wing. For the present case, oscillations about the midchord line of a nondeforming wing are considered.

Since $f(x,y)=\alpha(x-a)$ and, according to equation (3a),

$$w(x,y)=V\,\frac{\partial f(x,y)}{\partial x}+\frac{\partial f(x,y)}{\partial t}$$

then (for downwash, lift, and displacement positive in the same sense)

$$w(x,y)=-[V\alpha+\dot{\alpha}(x-a)]$$

and for harmonic motion

$$\frac{w(x,y)}{V\alpha}=-[1+ik(x-a)] \tag{A9}$$

It is convenient to divide the simultaneous equations by the factor $40/2\pi$ which appears in equation (30b). Therefore, the downwash conditions for rotation about midchord ($a=0$) are

$$\left.\begin{aligned}
&\frac{w(x_1,y_1)}{V\alpha}=\frac{w(x_4,y_4)}{V\alpha}=\frac{w(x_7,y_7)}{V\alpha}=-(0.025-0.00275i)2\pi\\
&\frac{w(x_2,y_2)}{V\alpha}=\frac{w(x_5,y_5)}{V\alpha}=\frac{w(x_8,y_8)}{V\alpha}=-(0.025+0i)2\pi\\
&\frac{w(x_3,y_3)}{V\alpha}=\frac{w(x_6,y_6)}{V\alpha}=\frac{w(x_9,y_9)}{V\alpha}=-(0.025+0.00275i)2\pi
\end{aligned}\right\} \tag{A10}$$

where x_i and y_i are the coordinates of the control points.

(6) By the use of the boundary condition $w/V\alpha$, the set of simultaneous equations (eqs. (A8)) may be solved for a_{nm}. For the example considered the values of the a_{nm} are

$$\left.\begin{aligned}
a_{00}&=-0.150858+0.033438i\\
a_{10}&=0.045628-0.129162i\\
a_{20}&=-0.000862-0.008337i\\
a_{02}&=-0.034965+0.007107i\\
a_{12}&=0.057334-0.031615i\\
a_{22}&=0.014221-0.004922i\\
a_{04}&=-0.025231+0.003860i\\
a_{14}&=0.058109-0.006198i\\
a_{24}&=0.045049-0.007729i
\end{aligned}\right\} \tag{A11}$$

(7) These coefficients may be used in equations (5) to determine the pressure distribution and, in turn, to obtain section forces, total forces, and so forth. The total lift and moment, for example, are given by equations (8) and (9) and for the sample case are

$$\left.\begin{aligned}
|C_{L,\alpha}|&=2.632 \qquad \phi_{L,\alpha}=194.43^\circ\\
|C_{M,\alpha}|&=1.594 \qquad \phi_{M,\alpha}=349.14^\circ
\end{aligned}\right\} \tag{A12}$$

APPENDIX B

TREATMENT OF CERTAIN INTEGRALS WHICH CONTAIN SINGULARITIES THAT ARISE IN THE CHORDWISE INTEGRATION

In the treatment of the chordwise integration in the surface-loading method, certain integrals arise which contain singularities (eqs. (16)) and which must be given special treatment. In the determination of the coefficients G_{rn} appearing in these equations, it is necessary to evaluate integrals of the form

$$I_n=\int_{chord} f_n(\xi)\overline{K}_{g\xi}\,d\xi \tag{B1}$$

where $f_n(\xi)$ is the nth typical chordwise pressure mode in the series expression for the continuous pressure distribution and $\overline{K}_{g\xi}=\overline{K}\,[M,k(x_g-\xi)]$ is the two-dimensional kernel function. In this equation, the kernel function becomes infinite at $\xi=x_g$ so that the integrand is singular. In the following sections, the methods of evaluating the integrals and taking care of the singularities are discussed. First the case of subsonic flow and then the case of sonic flow is discussed.

CASE OF SUBSONIC FLOW

For the case of subsonic flow, the integrals occurring in equations (16a) and (16b) are

$$I_0=\int_0^\pi \cot\frac{\theta}{2}\sin\theta\,\overline{K}_{g\xi}\,d\theta \tag{B2a}$$

$$I_n=\int_0^\pi \sin n\theta\sin\theta\,\overline{K}_{g\xi}\,d\theta \quad (n=1,2,\ldots) \tag{B2b}$$

Since the kernel in the integrands of I_0 and I_n becomes singular at $\xi=x_g$, it is necessary to separate the kernel into singular and nonsingular parts. The singular part can be integrated in closed analytic form. The nonsingular part can be handled routinely and accurately by numerical means. The separation of the singularity has been accomplished by Schwarz (ref. 34) in the following manner:

$$\overline{K}(M,Z)=\left[\frac{1}{Z}F(M)+iG(M)\log_e|Z|\right]+\overline{K}_1(M,Z) \tag{B3}$$

where

$$Z=k(x_g-\xi)$$

The singularities now appear only in the quantity in brackets, and the nonsingular part $\overline{K}_1$ has been tabulated by Schwarz (ref. 34). Substituting this expression into the integral of equation (B2a) gives (after setting $\xi=-\cos\theta$ and $x_g=-\cos\theta_o$)

$$\int_0^\pi \cot\frac{\theta}{2}\sin\theta\,\overline{K}(M,Z)d\theta=\int_0^\pi(1+\cos\theta)\overline{K}_1(M,Z)d\theta+\int_0^\pi(1+\cos\theta)\left[\frac{F(M)}{Z}+iG(M)\log_e|Z|\right]d\theta \tag{B4}$$

The first integral on the right-hand side of equation (B4) must be evaluated numerically. The second integral may be found analytically and has the following value:

$$\int_0^\pi(1+\cos\theta)\left[\frac{F(M)}{Z}+iG(M)\log_e|Z|\right]d\theta=\frac{\pi}{k}F(M)+iG(M)\left[-\pi\log_e 2-\pi\cos\theta_o+\pi\log_e k\right] \tag{B5}$$

The treatment of the integral of equation (B2b) for $n=1$ proceeds in a similar manner to yield

$$\int_0^\pi\sin^2\theta\,\overline{K}(M,Z)d\theta=\int_0^\pi\sin^2\theta\,K_1(M,Z)d\theta-\frac{\pi}{k}F(M)\cos\theta_o+\frac{i\pi}{2}G(M)\left(-\log_e 2+\frac{1}{2}\cos 2\theta_o+\log_e k\right) \tag{B6}$$

Correspondingly, for $n=2$,

$$\int_0^\pi\sin 2\theta\sin\theta\,\overline{K}(M,Z)d\theta=\int_0^\pi\sin 2\theta\sin\theta\,\overline{K}_1(M,Z)d\theta-\frac{\pi}{k}F(M)\cos 2\theta_o+\frac{i\pi}{2}G(M)\left(\frac{\cos 3\theta_o}{3}-\cos\theta_o\right) \tag{B7}$$

CASE OF SONIC FLOW

For the case of sonic flow, the form of the series expression for the chordwise loading and also the form of the kernel function differ from those of the subsonic case.

For $M=1$, the set of equations to be solved for the chordwise loads G_{rn} is given by equations (34) and (35). In equation (35), integrals of the following form appear:

$$I_n=\int_{-1}^{x_g}(1+\xi)^{n-\frac{1}{2}}\overline{K}_{g\xi}d\xi \qquad (n=0,1,2\ldots) \tag{B8}$$

At $M=1$, the two-dimensional kernel function appearing in these equations is given by equation (B23) of reference 24 and may be written as

$$\overline{K}_{g\xi}=\frac{2\sqrt{\pi}}{l}\left\{\frac{(1+i)ke^{-\frac{ikx_o}{2}}}{\sqrt{kx_o}}+(1-i)\sqrt{\pi}ke^{-ikx_o}\left[C\left(\sqrt{\frac{kx_o}{\pi}}\right)+iS\left(\sqrt{\frac{kx_o}{\pi}}\right)\right]\right\} \tag{B9}$$

where

$$x_o=x-\xi$$

and where $C\left(\sqrt{\frac{kx_o}{\pi}}\right)$ and $S\left(\sqrt{\frac{kx_o}{\pi}}\right)$ are Fresnel integrals defined by

$$C(\alpha)=\int_0^\alpha\cos\frac{\pi}{2}t^2dt$$

and

$$S(\alpha)=\int_0^\alpha\sin\frac{\pi t^2}{2}dt$$

As in the case of subsonic flow, the kernel function can be separated into singular and nonsingular parts. For this purpose, equation (B9) may be rewritten as

$$\overline{K}_{g\xi}\equiv(\overline{K}_{g\xi}-\overline{K}_{g\xi}')+\overline{K}_{g\xi}' \tag{B10}$$

where

$$\overline{K}_{g\xi}'=\frac{2\sqrt{\pi}}{l}(1+i)\frac{k}{\sqrt{kx_o}} \tag{B11}$$

so that

$$(\overline{K}_{g\xi}-\overline{K}_{g\xi}')=\frac{2\sqrt{\pi}}{l}\left\{\frac{(1+i)k}{\sqrt{kx_o}}\left(e^{-\frac{ikx_o}{2}}-1\right)+(1-i)\sqrt{\pi}ke^{-ikx_o}\left[C\left(\sqrt{\frac{kx_o}{\pi}}\right)+iS\left(\sqrt{\frac{kx_o}{\pi}}\right)\right]\right\} \tag{B12}$$

The integral I_n (eq. (B8)) can then be rewritten as

$$I_n=\int_{-1}^{x_g}(1+\xi)^{n-\frac{1}{2}}(\overline{K}_{g\xi}-\overline{K}_{g\xi}')d\xi+\int_{-1}^{x_g}(1+\xi)^{n-\frac{1}{2}}\overline{K}_{g\xi}'d\xi \tag{B13}$$

The first integral on the right of equation (B13) is nonsingular and can be evaluated numerically. The second integral contains a singularity and can be integrated analytically.

For $n=0$, the second integral on the right of equation (B13) is found to be

$$\int_{-1}^{x_g}\frac{K_{g\xi}'}{\sqrt{1+\xi}}d\xi=C\int_{-1}^{x_g}\frac{d\xi}{\sqrt{(1+\xi)(x_g-\xi)}}=C\pi \tag{B14}$$

where

$$C=\frac{2}{l}\sqrt{\frac{\pi}{k}}(1+i)k \tag{B15}$$

Correspondingly, for $n=1$, the integral becomes

$$C\int_{-1}^{x_g}\frac{\sqrt{1+\xi}}{\sqrt{x_g-\xi}}d\xi=C(x_g+1)\frac{\pi}{2} \tag{B16}$$

For $n=2$, there is obtained

$$C\int_{-1}^{x_g}\frac{(1+\xi)^{3/2}}{\sqrt{x_g-\xi}}d\xi=C(x_g+1)^2\frac{3\pi}{8} \tag{B17}$$

APPENDIX C

CALCULATION OF MOMENT ON DELTA WING

As mentioned in the text, the expression for the moment depends on the particular plan form. As an indication of the general method, the specific case of moment on a 45° delta wing is given in this appendix. The moment is calculated about a line $\xi=a$ as shown in sketch 3.

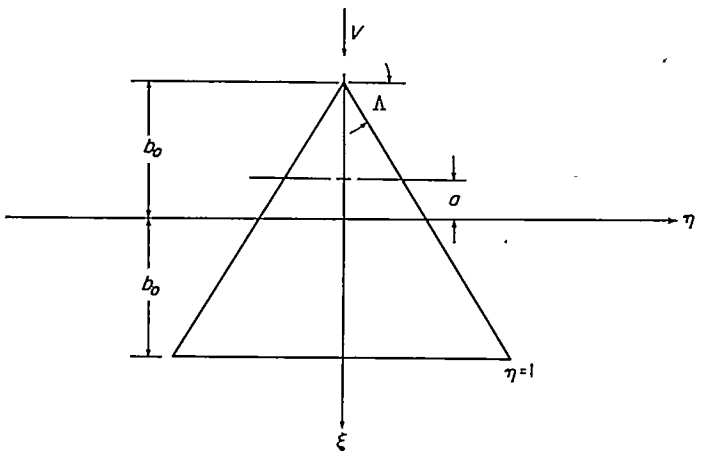

Sketch 3.

The expression for the moment as given by equation (7b) may be written as

$$M_\alpha=qSbC_{M,\alpha}=\iint_S(\xi-a)\Delta p_\alpha d\xi d\eta \tag{C1}$$

When equation (4) is used (for a 45° delta wing) the distance of an arbitrary point (η, ξ) from the line $\xi=a$ in terms of the variable θ is

$$\xi-a=s\left[\frac{\eta}{2}\tan\Lambda-\left(\frac{b_o}{s}-\frac{\eta}{2}\tan\Lambda\right)\cos\theta-a\frac{b_o}{s}\right] \tag{C2}$$

Substituting Δp (from eq. (5a)) and equation (C2) into equation (C1) and noting that

$$d\xi=s\left(\frac{b_o}{s}-\frac{\eta}{2}\tan\Lambda\right)\sin\theta\, d\theta=b(\eta)\sin\theta\, d\theta$$

results in the following:

$$M_\alpha=8s^3\rho V^2\int_0^1\int_0^\pi\sqrt{1-\eta^2}\left[\cot\frac{\theta}{2}(a_{00}+a_{02}\eta^2+a_{04}\eta^4)+\sin\theta(a_{10}+a_{12}\eta^2+a_{14}\eta^4)+\sin 2\theta(a_{20}+a_{22}\eta^2+a_{24}\eta^4)\right]\left[\frac{\eta}{2}\tan\Lambda-\left(\frac{b_o}{s}-\frac{\eta}{2}\tan\Lambda\right)\cos\theta-a\frac{b_o}{s}\right]\sin\theta\, d\theta\, d\eta \tag{C3}$$

In this example, three chordwise and three spanwise terms have been retained in the series for the loading Δp.

Performing the indicated integration in equation (C3) results in the following equation for the moment on a 45° delta wing $\left(\text{by making use of the fact that } \tan\Lambda=2\frac{b_o}{s}\right)$:

$$M_\alpha=8s^2b_o\rho V^2\pi\left[a_{00}\left(\frac{1}{2}-\frac{\pi}{8}-a\frac{\pi}{4}\right)+a_{02}\left(\frac{1}{5}-\frac{\pi}{32}-a\frac{\pi}{16}\right)+a_{04}\left(\frac{4}{35}-\frac{\pi}{64}-a\frac{\pi}{32}\right)+a_{10}\left(\frac{1}{6}-a\frac{\pi}{4}\right)+a_{12}\left(\frac{1}{15}-a\frac{\pi}{16}\right)+a_{14}\left(\frac{4}{105}-a\frac{\pi}{32}\right)+a_{20}\left(\frac{1}{12}-\frac{\pi}{16}\right)+a_{22}\left(\frac{1}{30}-\frac{\pi}{64}\right)+a_{24}\left(\frac{2}{105}-\frac{\pi}{128}\right)\right] \tag{C4}$$

APPENDIX D

DESCRIPTION OF A MULTIPLE-LINE METHOD

Since a lifting-line method of handling the integral equation (eq. (1)) may often be simpler than a lifting-surface procedure, it was considered interesting to investigate such a method and to compare results with those obtained by the surface approach. The purpose of this appendix is to present a lifting-line method based on a steady-state procedure developed by Schlichting and Kahlert (ref. 26) and to give some results obtained by it.

DESCRIPTION OF THE METHOD

In the Schlichting procedure for steady flow the lifting surface is divided into n spanwise strips of chord $c'=c/n$, where c is the total chord. A lifting line is placed at the ¼-chord position ($c'/4$) of each strip and the downwash is satisfied at control points on the ¾-chord position of each strip. This ¼-chord and ¾-chord location, respectively, of the lines and control points is an essential element of the procedure. It is a known fact that for a two-dimensional flat plate in steady incompressible flow the exact value of the lift can be obtained by placing a single lifting line at the ¼-chord position and satisfying the downwash at the ¾-chord position. Schlichting and Kahlert made use of this fact in developing a procedure for finite swept wings.

In adapting Schlichting's method to the oscillatory case the same placement of lifting lines and control points has been used and is shown in sketch 4, where, for example, the wing has been divided into two spanwise strips:

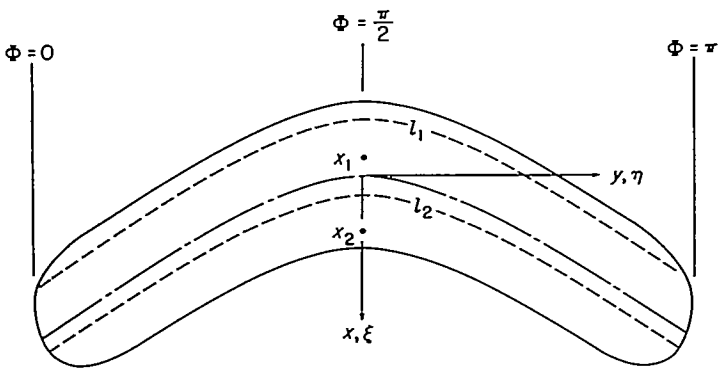

Sketch 4.

In this example two lifting lines l_1 and l_2 are considered that lie, respectively, at ⅛ and ⅝ of the total chord. Two control points are shown, by x_1 at ⅜c and x_2 at ⅞c. In the sketch Φ is an angular spanwise coordinate related to a nondimensional variable η (referred to the semispan) by $\eta=-\cos\Phi$.

In the original form of the integral equation given by equation (1), the continuous pressure distribution Δp is replaced by the sum of loadings on the individual lines. It is assumed that the loading on the line l_n can be represented by a series of the form

$$\Delta p_n=\rho V^2 s(a_{n1}\sin\Phi+a_{n3}\sin 3\Phi+a_{n5}\sin 5\Phi+\ldots) \qquad \text{(D1)}$$

which contains only one variable, the spanwise coordinate Φ. Since a separate loading function of this form is written for each lifting line, the double integration of equation (1) is reduced to a sum of single integrals. The integral equation then appears as

$$\frac{w(x,y)}{V}=\frac{1}{8\pi q s^2}\sum_n\int_{span}\Delta p_n\,\underline{K}[M,k(x-x_r),k(y-\eta)]\,d\eta \qquad \text{(D2)}$$

where x_r is the chordwise coordinate of the nth lifting line, and where $\underline{K}$, the nondimensional form of the kernel function defined by equation (28), has been employed.

When Δp_n in equation (D2) is replaced by the series expression in equation (D1), the integral equation is reduced to a summation of definite integrals multiplied by the coefficients a_{n1}, a_{n3}, and so forth, as follows:

$$\frac{w(x,y)}{V}=\frac{\rho V^2}{8\pi q s}\sum_n\left[a_{n1}\int_{-1}^{1}\sin\Phi\,\underline{K}(M,kx_o,ky_o)\,d\eta+a_{n3}\int_{-1}^{1}\sin 3\Phi\,\underline{K}(M,kx_o,ky_o)\,d\eta+\ldots\right] \qquad \text{(D3)}$$

where

$$x_o=x-x_r \qquad y_o=y-\eta$$

This equation sums the downwash at a particular control point due to all the lifting lines and the various types of loading, $\sin\Phi$, $\sin 3\Phi$, and so forth, on each line. The specific problem is the determination of the coefficients a_{n1}, a_{n3}, and so forth. In order to obtain the coefficients a, equation (D3) must be written for each of a number of control points. This leads to a set of simultaneous equations which can be solved for the values of a. At each control point the function $\frac{w(x,y)}{V}$ is determined from the motion of the wing in the same manner as in the surface-loading method.

Once the values of the coefficients a_{n1}, a_{n3}, and so forth, have been found, they can be used in equation (D1) to define the pressure distribution on any lifting line and in turn to give various force or moment coefficients. As an example, the total lift on a rectangular wing can be obtained from the relation

$$C_L=\frac{\sum_n L_n}{qS}=\frac{1}{qS}\sum_n\int_{-s}^{s}\Delta p_n\,dy \qquad \text{(D4)}$$

where L_n is the lift on the nth lifting line. The total pitching moment about an axis $x=a$ for a rectangular wing is given by

$$C_M=\frac{M_a}{qSb}$$
$$=\frac{1}{qS}\sum_n\left(\frac{x_n-a}{b}\right)L_n \tag{D5}$$

where x_n is the chordwise coordinate of the nth lifting line.

The main computational problem in the procedure is the evaluation of the spanwise integrals of equation (D3), and the handling of these integrals is discussed in the next section.

EVALUATION OF THE SPANWISE INTEGRALS

The spanwise integrations in equation (D3) are performed numerically and, since the kernel function has not been tabulated, it is necessary to make use of the series form of the kernel given by equations (31) and (54) of reference 24. In this form the nondimensional kernel function $\underline{K}$ appears as

$$\underline{K}(M,kx_o,ky_o)=e^{-ikx_o}\left\{-\left(\frac{\sqrt{x_o^2+\beta^2y_o^2}+x_o}{y_o^2\sqrt{x_o^2+\beta^2y_o^2}}\right)+\frac{ik}{\sqrt{x_o^2+\beta^2y_o^2}}+\frac{k^2}{2\beta^2}\left[M+\beta^2\left(\frac{1}{2}-\gamma\right)-\beta^2\log\frac{k}{2(1-M)}-\frac{\pi i\beta^2}{2}-\frac{x_o}{\sqrt{x_o^2+\beta^2y_o^2}}-\beta^2\log\left(\sqrt{x_o^2+\beta^2y_o^2}-x_o\right)\right]+0(k^3)\right\} \tag{D6}$$

where all distances are referred to the semispan s.

For the integrals of equation (D3) which relate to lifting lines behind the control point ($x_o<0$), the products of the loading modes and the kernel $\underline{K}$ as defined by equation (D4) can be evaluated at a number of values of η and the numerical integrations can be readily performed. When the lifting line lies ahead of the control point ($x_o>0$), however, the kernel becomes infinite at $\eta=y$, and the singularities must be carefully treated.

For the case $x_o>0$ with $\eta=y$, singularities arise in the terms

$$\left.\begin{aligned}A&=-\left(\frac{\sqrt{x_o^2+\beta^2y_o^2}+x_o}{y_o^2\sqrt{x_o^2+\beta^2y_o^2}}\right)\\ B&=-\frac{k^2}{2}\log\left(\sqrt{x_o^2+\beta^2y_o^2}-x_o\right)\end{aligned}\right\} \tag{D7}$$

Extraction of the singularities.—The singularities of the terms A and B can be extracted and, when combined with the loading terms $\sin\Phi$, $\sin 3\Phi$, and so forth, are integrable in closed form.

For this purpose, term A can be rewritten as

$$A=\left[-\left(\frac{\sqrt{x_o^2+\beta^2y_o^2}+x_o}{y_o^2\sqrt{x_o^2+\beta^2y_o^2}}\right)+\frac{2}{y_o^2}\right]-\frac{2}{y_o^2} \tag{D8}$$

where the quantity in brackets is finite for all values of η and where

$$\lim_{y\to 0}\left[-\left(\frac{\sqrt{x_o^2+\beta^2y_o^2}+x_o}{y_o^2\sqrt{x_o^2+\beta^2y_o^2}}\right)+\frac{2}{y_o^2}\right]=\frac{\beta^2}{2x_o^2} \tag{D9}$$

The remaining term on the right of equation (D8) contains the singularity and will be handled analytically.

The singularity of term B can also be isolated by writing

$$B=-\frac{k^2}{2}\log\left(\sqrt{x_o^2+\beta^2y_o^2}-x_o\right)=\left[\frac{k^2}{2}\log\left(\frac{\sqrt{x_o^2+\beta^2y_o^2}+x_o}{\beta^2}\right)\right]-\frac{k^2}{2}\log y_o^2 \tag{D10}$$

where the bracketed quantity is finite for all values of η and where the remaining term can be handled analytically.

Special form of the kernel for the case $x_o>0$.—The expressions for the terms A and B obtained in equations (D8) and (D10) can be used to define a special form of the kernel function for use in the case $x_o>0$. For this case the kernel can be written as

$$\underline{K}(M,kx_o,ky_o)_{x_o>0}=\underline{K}(x_o>0,y_o)+\underline{K}'(x_o>0,y_o) \tag{D11}$$

The term $\underline{K}(x_o>0,y_o)$ is nonsingular and is defined by

$$\underline{K}(x_o>0,y_o)=\underline{K}(M,kx_o,ky_o)+e^{-ikx_o}\left\{\frac{2}{y_o^2}+\frac{k^2}{2}\left[\log\left(\sqrt{x_o^2+\beta^2y_o^2}-x_o^2\right)+\log\left(\frac{\sqrt{x_o^2+\beta^2y_o^2}+x_o}{\beta^2}\right)\right]\right\} \tag{D12}$$

where $\underline{K}(M,k,x_o,y_o)$ is the form of the kernel defined by equation (D8).

The second term on the right-hand side of equation (D11) contains the singularities and is defined by

$$\underline{K}'(x_o>0,y_o)=-e^{-ikx_o}\left(\frac{2}{y_o^2}+\frac{k^2}{2}\log y_o^2\right) \tag{D13}$$

The form of the kernel given by equation (D11) is used in evaluating the integrals of equation (D3) for $x_o>0$.

Performance of the spanwise integrations.—It is recalled that for the case $x_o<0$, the integrals of equation (D3) can be readily evaluated numerically by making use of the form of the kernel given by equation (D8). For the case $x_o>0$, the integrals of equation (D3) can be handled by using the special form of the kernel defined by equation (D11). With this expression, a typical integral of equation (D3) for $x_o>0$ can be written as

$$\int_{-1}^{1}\sin m\Phi\,\underline{K}(M,kx_o,ky_o)_{x_o>0}\,d\eta=\int_{-1}^{1}\sin m\Phi\,\underline{K}(x_o>0,y_o)\,d\eta+\int_{-1}^{1}\sin m\Phi\,\underline{K}'(x_o>0,y_o)\,d\eta \tag{D14}$$

where the functions $\underline{K}(x_o>0,y_o)$ and $\underline{K}'(x_o>0,y_o)$ are defined, respectively, by equations (D12) and (D13). The first integral on the right of equation (D14) can be readily evaluated numerically. The second integral contains the singularities and must be evaluated analytically. Its values have been determined for two pressure modes, $\sin\Phi=\sqrt{1-\eta^2}$ and $\sin 3\Phi=(4\eta^2-1)\sqrt{1-\eta^2}$ and are

$$\int_{-1}^{1}\sqrt{1-\eta^2}\,\underline{K}'(x_o>0,y_o)\,d\eta=-e^{-ikx_o}\Big\{-2\pi+ k^2\sqrt{1-y^2}\,[(y+1)\log(y+1)-(y-1)\log(y-1)-2]+ \frac{k^2}{2}\int_{-1}^{1}(\sqrt{1-\eta^2}-\sqrt{1-y^2})\log y_o^2\,d\eta\Big\} \quad \text{(D15)}$$

and

$$\int_{-1}^{1}\sqrt{1-\eta^2}\,(4\eta^2-1)\underline{K}'(x_o>0,y_o)d\eta=-e^{-ikx_o}\Big\{-6\pi\frac{\sin 3\Phi_o}{\sin\Phi_o}+ k^2\sqrt{1-y^2}\,(4y^2-1)[(y+1)\log(y+1)-(y-1)\log(y-1)-2]+ \frac{k^2}{2}\int_{-1}^{1}[\sqrt{1-\eta^2}\,(4\eta^2-1)-\sqrt{1-y^2}\,(4y^2-1)]\log y_o^2 d\eta\Big\} \quad \text{(D16)}$$

where

$$\Phi_o=\cos^{-1}y$$

For the special case of a control point at $y=0$ and $x_o>0$, equation (D15) becomes

$$\int_{-1}^{1}\sqrt{1-\eta^2}\,\underline{K}'(x_o>0,-\eta)d\eta=-e^{-ikx_o}\left[-2\pi-\frac{k^2}{2}\left(\frac{\pi}{2}+\pi\log 2\right)\right] \quad \text{(D17)}$$

and equation (D16) becomes

$$\int_{-1}^{1}(4\eta^2-1)\sqrt{1-\eta^2}\,\underline{K}'(x_o>0,-\eta)d\eta=-e^{-ikx_o}\left[6\pi+\frac{k^2}{2}\left(\frac{3\pi}{4}\right)\right] \quad \text{(D18)}$$

For the case of $y\neq 0$ and $x_o>0$, the integrals remaining on the right of equations (D15) and (D16) are finite and can be evaluated numerically.

Once the integrals of equation (D3) have been evaluated, the simultaneous equations in terms of the unknown coefficients a_m, a_{n3}, and so forth, can be formed and solved in the manner indicated earlier. In the next section application of the multiple-line method is made and results are compared with those of the surface-loading method.

APPLICATION OF METHOD AND DISCUSSION OF RESULTS

The multiple-line method just discussed has been applied to the same rectangular wing with aspect ratio of 2 which was treated by the surface-loading method. Calculations have been made for several values of the reduced-frequency parameter k at $M=0$ for the wing oscillating in pitch about its midchord. Two sets of calculations were made, one using two lifting lines and two control points and the second using four lifting lines and eight control points. In the two sets of calculations, the control points were located chordwise in accordance with the ¾-chord concept discussed previously. With regard to spanwise location, in the first set of calculations, the two control points were placed at the center of the wing; in the second set of calculations, four control points were at the center of the wing and four at 0.866 semispan. Results of the calculations are shown in figure 6 as the lift and moment coefficients and their associated phase angles plotted against k. The results of the surface-loading method are included for comparison.

For the calculations of the lift based on two lines and two control points, the lift magnitude agrees well with the surface-loading results only at the lower frequencies. For the four-line, eight-point solution, results for the magnitude are approaching the results of the surface-loading method. Lift phase angles are in fairly good agreement for all sets of calculations.

With regard to the magnitude and phase angle of the moment, results of the line approach with four lines and eight control points are in fairly good agreement with those of the surface-loading method. There is significant improvement over the results of the two-line, two-control point calculations.

In general, it appears that in order to obtain accurate results with the multiple-line approach, a fairly large number of lifting lines and control points must be used.

REFERENCES

1. Cicala, P.: Comparison of Theory With Experiment in the Phenomenon of Wing Flutter. NACA TM 887, 1939.
2. Jones, W. P.: The Calculation of Aerodynamic Derivative Coefficients for Wings of Any Plan Form in Non-Uniform Motion. R. & M. No. 2470, British A.R.C., 1946.
3. Biot, M. A., and Boehnlein, C. T.: Aerodynamic Theory of the Oscillating Wing of Finite Span. GALCIT Rep. No. 5, Sept. 1942.
4. Reissner, Eric: Effect of Finite Span on the Airload Distributions for Oscillating Wings. I—Aerodynamic Theory of Oscillating Wings of Finite Span. NACA TN 1194, 1947.
5. Reissner, Eric, and Stevens, John E.: Effect of Finite Span on the Airload Distributions for Oscillating Wings. II—Methods of Calculation and Examples of Application. NACA TN 1195, 1947.
6. Jones, Robert T.: The Unsteady Lift of a Wing of Finite Aspect Ratio. NACA Rep. 681, 1940.
7. Küssner, H. G.: Theory of the Oscillating Airfoil of Large Aspect Ratio. Reps. and Translations No. 53, British M.A.P. Völkenrode, Apr. 15, 1946.
8. Laidlaw, W. R.: Theoretical and Experimental Pressure Distributions on Low Aspect Ratio Wings Oscillating in an Incompressible Flow. Tech. Rep. 51–2 (Contract NOas 52–576–c, Bur. Aero.), Aeroelastic and Structures Res. Lab., M.I.T., Sept. 1954.
9. Garrick, I. E., and Rubinow, S. I.: Theoretical Study of Air Forces on an Oscillating or Steady Thin Wing in a Supersonic Main Stream. NACA Rep. 872, 1947. (Supersedes NACA TN 1383.)

10. Miles, John W.: The Oscillating Rectangular Airfoil at Supersonic Speeds. Quarterly Appl. Math., vol. IX, no. 1, Apr. 1951, pp. 47–65.
11. Stewartson, K.: On Linearized Potential Theory of Unsteady Supersonic Motion. Quarterly Jour. Mech. and Appl. Math., vol. III, pt. 2, June 1950, pp. 182–199.
12. Nelson, Herbert C., Rainey, Ruby A., and Watkins, Charles E.: Lift and Moment Coefficients Expanded to the Seventh Power of Frequency for Oscillating Rectangular Wings in Supersonic Flow and Applied to a Specific Flutter Problem. NACA TN 3076, 1954.
13. Watkins, Charles E., and Berman, Julian H.: Air Forces and Moments on Triangular and Related Wings With Subsonic Leading Edges Oscillating in Supersonic Potential Flow. NACA Rep. 1099, 1952.
14. Watkins, Charles E., and Berman, Julian H.: Velocity Potential and Air Forces Associated With a Triangular Wing in Supersonic Flow, With Subsonic Leading Edges, and Deforming Harmonically According to a General Quadratic Equation. NACA TN 3009, 1953.
15. Merbt, H., and Landahl, M.: Aerodynamic Forces on Oscillating Low Aspect Ratio Wings in Compressible Flow. KTH Aero TN 30, Royal Inst. of Tech., Div. Aero. (Stockholm), 1953.
16. Voss, Herbert M., Zartarian, Garabed, and Hsu, Pao-Tan: Application of Numerical Integration Techniques to the Low-Aspect-Ratio Flutter Problem in Subsonic and Supersonic Flows. ASRL Tech. Rep. No. 52–3 (Contract No. NOa(s) 53–564–c), M.I.T., Oct. 1, 1954.
17. Reissner, Eric: On the Theory of Oscillating Airfoils of Finite Span in Subsonic Compressible Flow. NACA Rep. 1002, 1950. (Supersedes NACA TN 1953.)
18. Jones, W. P.: Oscillating Wings in Compressible Subsonic Flow. S. & C. 2560, British N.P.L. (Rep. No. 14,336, A.R.C.), Oct. 1951.
19. Lehrian, Doris E.: Calculation of Flutter Derivatives for Wings of General Plan-form. Rep. No. 16,445, British A.R.C., Jan. 1954.
20. Göthert, B.: Plane and Three-Dimensional Flow at High Subsonic Speeds. NACA TM 1105, 1946.
21. Miles, John W.: On the Compressibility Correction for Subsonic Unsteady Flow. Jour. Aero. Sci. (Readers' Forum), vol. 17, no. 3, Mar. 1950, pp. 181–182.
22. Schade, Th., and Krienes, K.: The Oscillating Circular Airfoil on the Basis of Potential Theory. NACA TM 1098, 1947.
23. Kuessner, H. G.: A General Method for Solving Problems of the Unsteady Lifting Surface Theory in the Subsonic Range. Jour. Aero. Sci., vol. 21, no. 1, Jan. 1954, pp. 17–26, 36.
24. Watkins, Charles E., Runyan, Harry L., and Woolston, Donald S.: On the Kernel Function of the Integral Equation Relating the Lift and Downwash Distributions of Oscillating Finite Wings in Subsonic Flow. NACA Rep. 1234, 1955. (Supersedes NACA TN 3131.)
25. Falkner, V. M.: The Calculation of Aerodynamic Loading on Surfaces of Any Shape. R. & M. No. 1910, British A.R.C., Aug. 1943.
26. Schlichting, H., and Kahlert, W.: On the Calculation of the Lift Distribution of Swept Wings. Rep. No. Aero. 2297, British R.A.E., Oct. 1948.
27. Fettis, Henry E.: An Approximate Method for the Calculation of Non-Stationary Air Forces at Subsonic Speeds. OAR Tech. Rep. No. 5 (ATI No. 99452), U. S. Air Force, Mar. 1951.
28. Lawrence, H. R.: The Lift Distribution on Low Aspect Ratio Wings at Subsonic Speeds. Jour. Aero. Sci., vol. 18, no. 10, Oct. 1951, pp. 683–695.
29. Lawrence, H. R., and Gerber, E. H.: The Aerodynamic Forces on Low Aspect Ratio Wings Oscillating in an Incompressible Flow. Jour. Aero. Sci., vol. 19, no. 11, Nov. 1952, pp. 769–781. (Errata issued, vol. 20, no. 4, Apr. 1953, p. 296.)
30. Multhopp, H.: Methods for Calculating the Lift Distribution of Wings (Subsonic Lifting Surface Theory). Rep. No. Aero. 2353, British R.A.E., Jan. 1950.
31. Weissinger, J.: The Lift Distribution of Swept-Back Wings. NACA TM 1120, 1947.
32. Jordan, Peter F.: On the Flutter of Swept Wings. Preprint No. 619, S.M.F. Fund Preprint, Inst. Aero. Sci., Jan. 1956.
33. Van Dorn, Nicholas H., and DeYoung, John: A Comparison of Three Theoretical Methods of Calculating Span Load Distribution on Swept Wings. NACA TN 1476, 1947. (Supersedes NACA RM A7C31.)
34. Schwarz, [L.]: Tables for the Calculation of Air Forces of the Vibrating Wing in Compressible Plane Subsonic Flow. AAF Translation No. F–TS–599–RE, Air Materiel Command, Aug. 1946.
35. Mangler, K. W.: Improper Integrals in Theoretical Aerodynamics. Rep. No. Aero. 2424, British R.A.E., June 1951.
36. Miles, John W.: On Linearized Theory. Jour. Aero. Sci. (Readers' Forum), vol. 20, no. 1, Jan. 1953, p. 64.
37. Mollo-Christensen, Erik L.: An Exploratory Investigation of Unsteady Transonic Flow. Part I—Theoretical Discussion. TACP Rep. 5 (Contract No. AF 33(038)–22184), M.I.T., Aero. Eng. Dept., June 1954.

TABLE I.—VALUES OF $G_{\nu n}$

[n=0, 1, 2; ν=1, 2, 3, 4]

(a) M=0

k	G_{10}	G_{20}	G_{30}	G_{40}
0				
0.02	1.718194+0.000616i	0.736332−0.000638i	0.441765−0.000412i	0.245302+0.000434i
0.06	1.719093+0.001479i	0.736393−0.001990i	0.441523−0.001162i	0.244586+0.001673i
0.10	1.720391+0.001845i	0.736438−0.003446i	0.441159−0.001816i	0.243605+0.003417i
0.20	1.724451+0.000670i	0.736223−0.007521i	0.439865−0.003040i	0.241054+0.009891i
0.30	1.728509−0.003131i	0.735275−0.012135i	0.438213−0.003732i	0.239596+0.018998i
0.40	1.731756−0.009046i	0.733421−0.017155i	0.436363−0.003983i	0.240053+0.030184i
0.50	1.733788−0.016615i	0.730576−0.022453i	0.434382−0.003864i	0.242847+0.042932i
0.60	1.734444−0.025452i	0.726706−0.027925i	0.432304−0.003417i	0.248139+0.056794i
0.70	1.733669−0.035272i	0.721815−0.033484i	0.430143−0.002693i	0.255966+0.071449i
0.80	1.731489−0.045854i	0.715925−0.039049i	0.427886−0.001712i	0.266293+0.086615i
0.90	1.727947−0.057051i	0.709075−0.044562i	0.425536−0.000490i	0.279033+0.102103i
1.00	1.723123−0.068755i	0.701300−0.049982i	0.423081+0.000968i	0.294089+0.117769i

k	G_{11}	G_{21}	G_{31}	G_{41}
0				
0.02	0.306807+0.001570i	0.478591+0.000403i	0.478591−0.000403i	0.306807−0.001570i
0.06	0.306843+0.004695i	0.478544+0.001204i	0.478548−0.001204i	0.306861−0.004695i
0.10	0.306916+0.007782i	0.478430+0.001998i	0.478448−0.001998i	0.307002−0.007782i
0.20	0.307109+0.015272i	0.477887+0.003932i	0.478021−0.003928i	0.307779−0.015276i
0.30	0.307572+0.022405i	0.476691+0.005807i	0.477265−0.005767i	0.309268−0.022445i
0.40	0.307077+0.029152i	0.475503+0.007562i	0.476441−0.007496i	0.311775−0.029218i
0.50	0.306637+0.035566i	0.473639+0.009263i	0.475337−0.009114i	0.315183−0.035715i
0.60	0.305858+0.041667i	0.471315+0.010902i	0.474033−0.010613i	0.319590−0.041956i
0.70	0.304718+0.047474i	0.468535+0.012481i	0.472541−0.011985i	0.325002−0.047970i
0.80	0.303222+0.053011i	0.465307+0.014008i	0.470852−0.013224i	0.331415−0.053795i
0.90	0.301382+0.058287i	0.461644+0.015488i	0.468970−0.014325i	0.338800−0.059450i
1.00	0.299211+0.063309i	0.457560+0.016922i	0.466894−0.015278i	0.347131−0.064953i

k	G_{12}	G_{22}	G_{32}	G_{42}
0				
0.02	0.460172+0.001446i	0.239286−0.000715i	−0.239286−0.000717i	−0.460172+0.000712i
0.06	0.460089+0.002179i	0.239261−0.002140i	−0.239261−0.002154i	−0.460089+0.002115i
0.10	0.459935+0.003665i	0.239193−0.003559i	−0.239193−0.003595i	−0.459935+0.003489i
0.20	0.459303+0.007477i	0.238877−0.007074i	−0.238872−0.007208i	−0.459308+0.006805i
0.30	0.458392+0.011394i	0.238383−0.010540i	−0.238368−0.010824i	−0.458407+0.009970i
0.40	0.457251+0.015372i	0.237728−0.013954i	−0.237693−0.014422i	−0.457286+0.013004i
0.50	0.455894+0.019375i	0.236911−0.017309i	−0.236849−0.017992i	−0.455956+0.015926i
0.60	0.454331+0.023372i	0.235937−0.020601i	−0.235838−0.021518i	−0.454430+0.018747i
0.70	0.452569+0.027335i	0.234811−0.023827i	−0.234665−0.024981i	−0.452715+0.021473i
0.80	0.450610+0.031244i	0.233530−0.026976i	−0.233331−0.028378i	−0.450809+0.024110i
0.90	0.448453+0.035083i	0.232102−0.030047i	−0.231838−0.031696i	−0.448717+0.026660i
1.00	0.446108+0.038835i	0.230529−0.033030i	−0.230195−0.034923i	−0.446442+0.029118i

TABLE I.—VALUES OF G_{rn}—Continued

(b) $M=0.5$

k	G_{10}	G_{20}	G_{30}	G_{40}
0.02	1.718217+0.000834i	0.736335−0.000849i	0.441762−0.000551i	0.245279+0.000565i
0.04	1.718621+0.001532i	0.736387−0.001721i	0.441645−0.001075i	0.244937+0.001265i
0.06	1.719202+0.002088i	0.736390−0.002623i	0.441498−0.001571i	0.244506+0.002106i
0.08	1.719851+0.002505i	0.736400−0.003556i	0.441332−0.002037i	0.244010+0.003088i
0.10	1.720582+0.002796i	0.736408−0.004513i	0.441132−0.002479i	0.243471+0.004196i
0.12	1.721371+0.002941i	0.736408−0.005492i	0.440915−0.002896i	0.242899+0.005447i
0.14	1.722223+0.002936i	0.736379−0.006502i	0.440675−0.003278i	0.242316+0.006844i
0.16	1.723147+0.002795i	0.736308−0.007647i	0.440405−0.003672i	0.241733+0.008524i
0.18	1.723962+0.002564i	0.736244−0.008599i	0.440155−0.003969i	0.241262+0.010005i
0.20	1.724866+0.002177i	0.736099−0.009688i	0.439865−0.004274i	0.240763+0.011785i
0.30	1.728804−0.001338i	0.735006−0.015459i	0.438406−0.005496i	0.239377+0.022294i
0.40	1.731636−0.007179i	0.732954−0.021727i	0.436931−0.006275i	0.240072+0.035181i
0.50	1.732840−0.014669i	0.729879−0.028394i	0.435561−0.0067054i	0.243313+0.049768i

k	G_{11}	G_{21}	G_{31}	G_{41}
0.02	0.306817+0.002095i	0.478588+0.000537i	0.478584−0.000537i	0.306807−0.002094i
0.04	0.306838+0.004182i	0.478561+0.001072i	0.478559−0.001072i	0.306838−0.004182i
0.06	0.306892+0.006258i	0.478498+0.001606i	0.478500−0.001606i	0.306906−0.006258i
0.08	0.306955+0.008320i	0.478403+0.002137i	0.478417−0.002136i	0.307021−0.008321i
0.10	0.307026+0.010375i	0.478293+0.002666i	0.478317−0.002664i	0.307160−0.010378i
0.12	0.307102+0.012407i	0.478152+0.003192i	0.478201−0.003191i	0.307341−0.012408i
0.14	0.307197+0.014415i	0.477988+0.003711i	0.478061−0.003711i	0.307550−0.014415i
0.16	0.307297+0.016605i	0.477771+0.004280i	0.477885−0.004279i	0.307843−0.016606i
0.18	0.307389+0.018381i	0.477573+0.004743i	0.477720−0.004741i	0.308114−0.018382i
0.20	0.307493+0.020326i	0.477327+0.005250i	0.477520−0.005249i	0.308456−0.020328i
0.30	0.307896+0.029804i	0.475616+0.007738i	0.476247−0.007751i	0.311037−0.029792i
0.40	0.308056+0.038807i	0.473175+0.010123i	0.474563−0.010171i	0.315002−0.038759i
0.50	0.307873+0.047441i	0.469953+0.012440i	0.472474−0.012526i	0.320496−0.047355i

k	G_{12}	G_{22}	G_{32}	G_{42}
0.02	0.460170+0.000958i	0.239281−0.000954i	−0.239283−0.000955i	−0.460168+0.000951i
0.04	0.460136+0.001924i	0.239276−0.001906i	−0.239279−0.001911i	−0.460133+0.001893i
0.06	0.460062+0.002898i	0.239239−0.002856i	−0.239245−0.002870i	−0.460056+0.002828i
0.08	0.459969+0.003882i	0.239191−0.003806i	−0.239191−0.003831i	−0.459969+0.003754i
0.10	0.459857+0.004870i	0.239132−0.004754i	−0.239133−0.004792i	−0.459856+0.004675i
0.12	0.459720+0.005869i	0.239058−0.005700i	−0.239051−0.005756i	−0.459727+0.005587i
0.14	0.459570+0.006871i	0.238974−0.006643i	−0.238967−0.006720i	−0.459577+0.006492i
0.16	0.459372+0.007981i	0.238861−0.007679i	−0.238857−0.007782i	−0.459376+0.007480i
0.18	0.459211+0.008896i	0.238757−0.008528i	−0.238763−0.008650i	−0.459205+0.008282i
0.20	0.459017+0.009915i	0.238632−0.009464i	−0.238647−0.009619i	−0.459002+0.009169i
0.30	0.457749+0.015086i	0.237839−0.014157i	−0.237842−0.014470i	−0.457746+0.013542i
0.40	0.456166+0.020323i	0.236761−0.018815i	−0.236783−0.019317i	−0.456144+0.017809i
0.50	0.454244+0.025623i	0.235398−0.023459i	−0.235440−0.024159i	−0.454202+0.021995i

TABLE I.—VALUES OF G_{rn}—Concluded

(c) $M=1.0$

k	G_{10}	G_{20}	G_{30}	G_{40}
0. 10	2. 220453+0. 024422i	0. 938021+0. 048128i	0. 684779+0. 057930i	0. 156747−0. 130480i
0. 12	2. 219995+0. 029881i	0. 937372+0. 057824i	0. 684637+0. 070004i	0. 157996−0. 157709i
0. 16	2. 218702+0. 039212i	0. 936469+0. 076523i	0. 683875+0. 092470i	0. 160954−0. 208205i
0. 198675	2. 217279+0. 049746i	0. 935663+0. 096413i	0. 677372+0. 117037i	0. 169686−0. 263196i
0. 242825	2. 215455+0. 059393i	0. 948201+0. 103049i	0. 674169+0. 149419i	0. 162175−0. 311861i
0. 286975	2. 212373+0. 070518i	0. 930797+0. 136024i	0. 679618+0. 166138i	0. 177212−0. 372680i

k	G_{11}	G_{21}	G_{31}	G_{41}
0. 10	0. 277575+0. 005300i	0. 394836+0. 009153i	0. 480561+0. 012698i	0. 180361−0. 027151i
0. 12	0. 277517+0. 006386i	0. 394828+0. 010933i	0. 480658+0. 015433i	0. 180330−0. 032752i
0. 16	0. 277390+0. 008396i	0. 394583+0. 014674i	0. 480234+0. 020595i	0. 181126−0. 043665i
0. 198675	0. 277234+0. 010424i	0. 394336+0. 018212i	0. 479269+0. 025485i	0. 182494−0. 054121i
0. 242825	0. 277012+0. 012734i	0. 393992+0. 022239i	0. 479517+0. 031221i	0. 182812−0. 066194i
0. 286975	0. 276750+0. 015034i	0. 393575+0. 026266i	0. 479018+0. 036870i	0. 183990−0. 078170i

k	G_{12}	G_{22}	G_{32}	G_{42}
0. 10	0. 052035+0. 001315i	0. 178118+0. 004118i	0. 342280+0. 008298i	0. 227567−0. 013731i
0. 12	0. 052030+0. 001571i	0. 178064+0. 004925i	0. 342163+0. 009993i	0. 227743−0. 016489i
0. 16	0. 051996+0. 002091i	0. 177993+0. 006633i	0. 342012+0. 013405i	0. 227999−0. 022129i
0. 198675	0. 051964+0. 002595i	0. 177877+0. 008233i	0. 341668+0. 016622i	0. 228491−0. 027450i
0. 242825	0. 051914+0. 003170i	0. 177719+0. 010056i	0. 341484+0. 020322i	0. 228883−0. 033548i
0. 286975	0. 051855+0. 003742i	0. 177528+0. 011878i	0. 341115+0. 023999i	0. 229502−0. 039619i

TABLE II.—VALUES OF $G_{\nu n}\mu^m\sqrt{1-\mu^2}$ FOR THE SAMPLE CASE OF APPENDIX A

[$M=0.5$; $k=0.22$]

ν	μ	$G_{\nu 0}\sqrt{1-\mu^2}$	$G_{\nu 1}\sqrt{1-\mu^2}$	$G_{\nu 2}\sqrt{1-\mu^2}$	$G_{\nu 0}\mu^2\sqrt{1-\mu^2}$	$G_{\nu 1}\mu^2\sqrt{1-\mu^2}$	$G_{\nu 2}\mu^2\sqrt{1-\mu^2}$	$G_{\nu 0}\mu^4\sqrt{1-\mu^2}$	$G_{\nu 1}\mu^4\sqrt{1-\mu^2}$	$G_{\nu 2}\mu^4\sqrt{1-\mu^2}$
1	0	1.72184+0.00294i	0.30752+0.02241i	0.45744+0.01103i	0 +0i	0 +0i	0 +0i	0 +0i	0 +0i	0 +0i
	0.1	1.71321+0.00223i	0.30596+0.02220i	0.45515+0.01096i	0.01713+0.00002i	0.00306+0.00022i	0.00455+0.00011i	0.00017+0i	0.00003+0i	0.00005+0i
	0.2	1.68705+0.00200i	0.30131+0.02194i	0.44820+0.01061i	0.06748+0.00009i	0.01205+0.00068i	0.01793+0.00043i	0.00270+0i	0.00048+0.00004i	0.00072+0.00002i
	0.3	1.64253+0.00214i	0.29336+0.02128i	0.43637+0.01053i	0.14753+0.00019i	0.02640+0.00192i	0.03927+0.00096i	0.01350+0.00002i	0.00238+0.00017i	0.00353+0.00009i
	0.4	1.57800+0.00206i	0.28185+0.02054i	0.41925+0.01011i	0.25249+0.00033i	0.04510+0.00329i	0.06708+0.00162i	0.04040+0.00005i	0.00722+0.00053i	0.01073+0.00026i
	0.5	1.49116+0.00194i	0.26632+0.01941i	0.39615+0.00956i	0.37279+0.00048i	0.06668+0.00485i	0.09904+0.00239i	0.09330+0.00012i	0.01664+0.00121i	0.02476+0.00060i
	0.6	1.37747+0.00180i	0.24602+0.01793i	0.36595+0.00883i	0.49589+0.00065i	0.08857+0.00645i	0.13174+0.00318i	0.17852+0.00023i	0.03189+0.00232i	0.04743+0.00114i
	0.7	1.22964+0.00160i	0.21961+0.01601i	0.32363+0.00788i	0.60259+0.00078i	0.10761+0.00784i	0.16007+0.00386i	0.26523+0.00038i	0.05273+0.00384i	0.07843+0.00189i
	0.8	1.03310+0.00135i	0.18451+0.01345i	0.27446+0.00662i	0.68118+0.00088i	0.11809+0.00861i	0.17565+0.00424i	0.42316+0.00055i	0.07566+0.00551i	0.11243+0.00271i
	0.9	0.76053+0.00098i	0.13404+0.00977i	0.19939+0.00481i	0.60793+0.00079i	0.10357+0.00791i	0.16151+0.00390i	0.49242+0.00064i	0.08794+0.00641i	0.13039+0.00316i
2	0	0.73737−0.01130i	0.47670+0.00862i	0.23804−0.01056i	0 +0i	0 +0i	0 +0i	0 +0i	0 +0i	0 +0i
	0.1	0.73357−0.01124i	0.47431+0.00830i	0.23685−0.01050i	0.00734−0.00011i	0.00474+0.00006i	0.00237−0.00010i	0.00007+0i	0.00005+0i	0.00009+0i
	0.2	0.72247−0.01107i	0.46707+0.00771i	0.23323−0.01033i	0.02890−0.00044i	0.01868+0.00023i	0.00933−0.00041i	0.00116−0.00002i	0.00075+0.00001i	0.00037−0.00002i
	0.3	0.70341−0.01078i	0.45474+0.00656i	0.22708−0.01006i	0.06331−0.00097i	0.04093+0.00050i	0.09044−0.00091i	0.00570−0.00009i	0.00368+0.00004i	0.00184−0.00008i
	0.4	0.67561−0.01038i	0.43690+0.00534i	0.21817−0.00967i	0.10813−0.00166i	0.06990+0.00085i	0.09491−0.00155i	0.01730−0.00027i	0.01118+0.00014i	0.00559−0.00025i
	0.5	0.63866−0.00979i	0.41283+0.00504i	0.20615−0.00913i	0.15964−0.00245i	0.10321+0.00126i	0.05154−0.00228i	0.03991−0.00061i	0.02580+0.00031i	0.01288−0.00067i
	0.6	0.58990−0.00904i	0.38136+0.00466i	0.19043−0.00844i	0.21236−0.00325i	0.13729+0.00168i	0.06855−0.00304i	0.07645−0.00117i	0.04942−0.00060i	0.02468−0.00109i
	0.7	0.52659−0.00807i	0.34043+0.00416i	0.16999−0.00753i	0.25603−0.00396i	0.16061+0.00204i	0.08330−0.00369i	0.12543−0.00194i	0.08174+0.00100i	0.04032−0.00181i
	0.8	0.44942−0.00678i	0.28609+0.00350i	0.14282−0.00633i	0.28315−0.00434i	0.18305+0.00224i	0.09140−0.00406i	0.18122−0.00278i	0.11715+0.00143i	0.05850−0.00259i
	0.9	0.32141−0.00493i	0.20770+0.00254i	0.10376−0.00460i	0.25034−0.00309i	0.18831+0.00206i	0.08405−0.00373i	0.21088−0.00323i	0.13633+0.00107i	0.06808−0.00302i
3	0	0.44062−0.00484i	0.47702−0.00863i	−0.23753−0.01073i	0 +0i	0 +0i	0 +0i	0 +0i	0 +0i	0 +0i
	0.1	0.43831−0.00481i	0.47453−0.00581i	−0.23634−0.01007i	0.00438−0.00005i	0.00475−0.00006i	−0.00236−0.00011i	0.00004+0i	0.00005+0i	−0.00002+0i
	0.2	0.43162−0.00474i	0.46738−0.00572i	−0.23273−0.01051i	0.01726−0.00019i	0.01870−0.00023i	−0.00931−0.00042i	0.00069−0.00001i	0.00075−0.00001i	−0.00037−0.00002i
	0.3	0.42023−0.00462i	0.45505−0.00557i	−0.22569−0.01023i	0.03782−0.00042i	0.04095−0.00050i	−0.03039−0.00092i	0.00340−0.00004i	0.00389−0.00004i	−0.00184−0.00008i
	0.4	0.40374−0.00443i	0.43720−0.00535i	−0.21770−0.00983i	0.06460−0.00071i	0.06995−0.00085i	−0.03483−0.00157i	0.01034−0.00011i	0.01119−0.00014i	−0.00557−0.00025i
	0.5	0.38150−0.00419i	0.41311−0.00505i	−0.20671−0.00929i	0.09537−0.00105i	0.10323−0.00126i	−0.03143−0.00233i	0.02384−0.00026i	0.02582−0.00031i	−0.01286−0.00058i
	0.6	0.35242−0.00387i	0.38162−0.00467i	−0.19002−0.00858i	0.12687−0.00139i	0.13738−0.00168i	−0.06841−0.00309i	0.04567−0.00050i	0.04946−0.00060i	−0.02463−0.00111i
	0.7	0.31459−0.00345i	0.34060−0.00417i	−0.16963−0.00766i	0.15415−0.00170i	0.16692−0.00204i	−0.08312−0.00378i	0.07563−0.00083i	0.08179−0.00100i	−0.04078−0.00184i
	0.8	0.26431−0.00290i	0.28621−0.00350i	−0.14262−0.00644i	0.16916−0.00185i	0.18317−0.00224i	−0.09121−0.00412i	0.10396−0.00119i	0.11723−0.00143i	−0.05837−0.00264i
	0.9	0.19202−0.00211i	0.20793−0.00254i	−0.10354−0.00468i	0.15554−0.00171i	0.16842−0.00206i	−0.08387−0.00379i	0.12599−0.00139i	0.13642−0.00167i	−0.06793−0.00307i
4	0	0.24180+0.01382i	0.30950−0.02240i	−0.45795+0.01024i	0 +0i	0 +0i	0 +0i	0 +0i	0 +0i	0 +0i
	0.1	0.24065+0.01382i	0.30801−0.02229i	−0.45665+0.01019i	0.00941+0.00014i	0.00308−0.00022i	−0.00456+0.00010i	0.00002+0i	0.00003+0i	−0.00005+0i
	0.2	0.23697+0.01361i	0.30331−0.02195i	−0.44869+0.01003i	0.03948+0.00054i	0.01213−0.00088i	−0.01795+0.00040i	0.00038−0.00002i	0.00049−0.00004i	−0.00072+0.00002i
	0.3	0.23072+0.01325i	0.29530−0.02137i	−0.43366+0.00977i	0.02070+0.00119i	0.02068−0.00192i	−0.03932+0.00088i	0.00187−0.00011i	0.00239−0.00017i	−0.00354+0.00034i
	0.4	0.22167+0.01273i	0.28372−0.02053i	−0.41972+0.00939i	0.03547−0.00203i	0.04540−0.00328i	−0.06716+0.00150i	0.00563−0.00032i	0.00720−0.00052i	−0.01075+0.00064i
	0.5	0.20940+0.01203i	0.26800−0.01940i	−0.39660+0.00887i	0.05236−0.00301i	0.06702−0.00485i	−0.09915+0.00222i	0.01309−0.00075i	0.01675−0.00121i	−0.02479+0.00055i
	0.6	0.19340+0.01112i	0.24765−0.01792i	−0.36630+0.00819i	0.06966−0.00400i	0.08915−0.00645i	−0.13180+0.00296i	0.02503+0.00144i	0.03209−0.00232i	−0.04748+0.00106i
	0.7	0.17272+0.00992i	0.22107−0.01600i	−0.32704+0.00731i	0.08463−0.00488i	0.10832−0.00784i	−0.16025+0.00358i	0.04147−0.00238i	0.05308−0.00384i	−0.07852+0.00175i
	0.8	0.14512+0.00834i	0.18574−0.01344i	−0.27477+0.00614i	0.09288+0.00534i	0.11887−0.00860i	−0.17585+0.00393i	0.06944+0.00342i	0.07008−0.00550i	−0.11254+0.00252i
	0.9	0.10542+0.00606i	0.13493−0.00977i	−0.19962+0.00446i	0.08539+0.00491i	0.10929−0.00701i	−0.16169+0.00361i	0.06917+0.00396i	0.06862−0.00641i	−0.13097+0.00292i

TABLE III.—VALUES OF THE DOWNWASH FACTORS F_R+F_L FOR THE NINE CONTROL POINTS OF THE SAMPLE CASE OF APPENDIX A

[M=0.5; k=0.22]

ν	μ	Control point 1	Control point 2	Control point 3	Control point 4	Control point 5	Control point 6	Control point 7	Control point 8	Control point 9
1	0	−0.21173+0.02131i	−0.24927+0.04610i	−0.24974+0.07324i	−0.00834+0.00293i	−0.01027+0.00388i	−0.01134+0.00407i	−0.02453+0.00560i	−0.03147+0.00843i	−0.03377+0.01188i
	0.1	−1.32029+0.09338i	−1.40044+0.23834i	−1.37920+0.39466i	−0.01780+0.00600i	−0.02188+0.00802i	−0.02411+0.01035i	−0.05724+0.01190i	−0.07318+0.01853i	−0.07775+0.02652i
	0.2	4.07351−0.20244i	3.91060−0.64237i	3.80353−1.06782i	−0.02095+0.00648i	−0.02642+0.00891i	−0.02888+0.01173i	−0.06180+0.01492i	−0.11514+0.02174i	−0.11932+0.03134i
	0.3	−1.28418+0.06754i	−1.33006+0.22986i	−1.30924+0.37450i	−0.02840+0.00744i	−0.03613+0.01070i	−0.03904+0.01403i	−0.07923+0.02423i	−0.25954+0.06004i	−0.26106+0.07821i
	0.4	−0.22783+0.02564i	−0.25977−0.05337i	−0.27205+0.06165i	−0.04428+0.00922i	−0.05641+0.01445i	−0.06963+0.02053i	−1.24590+0.08447i	−1.30718+0.23463i	−1.28396+0.36677i
	0.5	−0.09189+0.01492i	−0.11514+0.02174i	−0.11932+0.03324i	−0.06321+0.01288i	−0.10309+0.01969i	−0.10709+0.03400i	4.10980−0.20785i	3.96755−0.65209i	3.85250−1.09260i
	0.6	−0.04939+0.01049i	−0.00204+0.01630i	−0.06670+0.02308i	−0.21390+0.02264i	−0.25177+0.04774i	−0.25249+0.07508i	−1.24352+0.08386i	−1.30414+0.23374i	−1.28003+0.35556i
	0.7	−0.03078+0.00805i	−0.03916+0.01104i	−0.04229+0.01584i	−1.24143+0.08318i	−1.30156+0.22283i	−1.27775+0.38437i	−0.21486+0.02297i	−0.25300+0.04818i	−0.25387+0.07586i
	0.8	−0.02095+0.00648i	−0.02542+0.00891i	−0.02888+0.01173i	4.11310−0.20691i	3.96173−0.65353i	3.85715−1.08448i	−0.03321+0.01288i	−0.10390+0.01850i	−0.10709+0.03400i
	0.9	−0.01512+0.00539i	−0.01884+0.00714i	−0.02076+0.00914i	−1.24003+0.08297i	−1.30096+0.22256i	−1.27708+0.38404i	−0.04328+0.00889i	−0.05517+0.01400i	−0.05620+0.01995i
2	0	−0.06146+0.00661i	−0.21173+0.02131i	−0.24927+0.04616i	−0.00507+0.00215i	−0.00834+0.00203i	−0.01027+0.00388i	−0.01363+0.00345i	−0.02453+0.00556i	−0.03147+0.00843i
	0.1	−0.11869+0.01414i	−1.32029+0.09338i	−1.40044+0.23834i	−0.01183+0.00437i	−0.01780+0.00600i	−0.02188+0.00802i	−0.02966+0.00710i	−0.05724+0.01190i	−0.07318+0.01853i
	0.2	−0.13519+0.01437i	4.07351−0.20244i	3.91060−0.64237i	−0.01341+0.00458i	−0.02095+0.00648i	−0.02642+0.00891i	−0.03815+0.00774i	−0.06180+0.01492i	−0.11514+0.02174i
	0.3	−0.10152+0.01233i	−1.28418+0.06754i	−1.33006+0.22986i	−0.01656+0.00495i	−0.02840+0.00744i	−0.03613+0.01070i	−0.05713+0.00906i	−0.21968+0.03423i	−0.25964+0.06004i
	0.4	−0.06128+0.00971i	−0.22783+0.02564i	−0.25977−0.05337i	−0.02228+0.00556i	−0.04428+0.00922i	−0.05641+0.01445i	−0.09236+0.01077i	−1.24590+0.08447i	−1.30718+0.23463i
	0.5	−0.03815+0.00774i	−0.09189+0.01492i	−0.11514+0.02174i	−0.03282+0.00948i	−0.06321+0.01288i	−0.10309+0.01969i	−0.11895+0.01185i	4.10980−0.20785i	3.96755−0.65209i
	0.6	−0.02561+0.00635i	−0.04939+0.01049i	−0.06204+0.01630i	−0.05316+0.00792i	−0.21390+0.02264i	−0.25177+0.04774i	−0.09083+0.01038i	−1.24352+0.08386i	−1.30414+0.23374i
	0.7	−0.01809+0.00534i	−0.03078+0.00805i	−0.03916+0.01164i	−0.08635+0.00990i	−1.24143+0.08318i	−1.30156+0.22283i	−0.06388+0.00616i	−0.21486+0.02297i	−0.25300+0.04818i
	0.8	−0.01341+0.00458i	−0.02095+0.00648i	−0.02542+0.00891i	−0.11600+0.01110i	4.11310−0.20691i	3.96173−0.65353i	−0.03333+0.00448i	−0.03321+0.01288i	−0.10390+0.01850i
	0.9	−0.01028+0.00398i	−0.01512+0.00539i	−0.01884+0.00714i	−0.08896+0.00974i	−1.24003+0.08297i	−1.30096+0.22256i	−0.02156+0.00531i	−0.04328+0.00889i	−0.05517+0.01400i
3	0	−0.01074+0.00284i	−0.06146+0.00661i	−0.21173+0.02131i	−0.00347+0.00156i	−0.00507+0.00215i	−0.00834+0.00203i	−0.00921+0.00213i	−0.01362+0.00345i	−0.02453+0.00556i
	0.1	−0.02115+0.00563i	−0.11869+0.01414i	−1.32029+0.09338i	−0.00709+0.00314i	−0.01182+0.00437i	−0.01780+0.00600i	−0.01267+0.00428i	−0.02966+0.00710i	−0.05724+0.01190i
	0.2	−0.02006+0.00544i	−0.13519+0.01437i	4.07351−0.20244i	−0.00753+0.00321i	−0.01341+0.00458i	−0.02095+0.00648i	−0.01333+0.00434i	−0.03815+0.00774i	−0.06180+0.01492i
	0.3	−0.01823+0.00615i	−0.10152+0.01233i	−1.28418+0.06754i	−0.00627+0.00331i	−0.01656+0.00495i	−0.02840+0.00744i	−0.01421+0.00440i	−0.05712+0.00906i	−0.21968+0.03423i
	0.4	−0.01583+0.00476i	−0.06128+0.00971i	−0.22783+0.02564i	−0.00933+0.00344i	−0.02226+0.00556i	−0.04428+0.00922i	−0.01490+0.00443i	−0.09236+0.01077i	−1.24590+0.08447i
	0.5	−0.01333+0.00434i	−0.03815+0.00774i	−0.09189+0.01492i	−0.01064+0.00360i	−0.03282+0.00948i	−0.06321+0.01288i	−0.01493+0.00436i	−0.11895+0.01185i	4.10980−0.20785i
	0.6	−0.01105+0.00393i	−0.02561+0.00635i	−0.04939+0.01049i	−0.01204+0.00376i	−0.05316+0.00792i	−0.21390+0.02264i	−0.01406+0.00419i	−0.09083+0.01038i	−1.24352+0.08386i
	0.7	−0.00911+0.00356i	−0.01809+0.00534i	−0.03078+0.00805i	−0.01312+0.00386i	−0.08635+0.00990i	−1.24143+0.08318i	−0.01240+0.00392i	−0.06388+0.00616i	−0.21486+0.02297i
	0.8	−0.00753+0.00321i	−0.01341+0.00458i	−0.02095+0.00648i	−0.01347+0.00386i	−0.11600+0.01110i	4.11310−0.20691i	−0.01064+0.00360i	−0.03332+0.00448i	−0.06321+0.01288i
	0.9	−0.00625+0.00290i	−0.01028+0.00398i	−0.01512+0.00539i	−0.01280+0.00374i	−0.08896+0.00974i	−1.24003+0.08297i	−0.00889+0.00338i	−0.02156+0.00531i	−0.04328+0.00889i
4	0	−0.00394+0.00163i	−0.01074+0.00284i	−0.06146+0.00661i	−0.00209+0.00115i	−0.00347+0.00156i	−0.00507+0.00215i	−0.00300+0.00140i	−0.00621+0.00213i	−0.01362+0.00345i
	0.1	−0.00790+0.00323i	−0.02115+0.00563i	−0.11869+0.01414i	−0.00415+0.00230i	−0.00709+0.00314i	−0.01183+0.00437i	−0.00800+0.00290i	−0.01267+0.00428i	−0.02966+0.00710i
	0.2	−0.00753+0.00316i	−0.02006+0.00544i	−0.13519+0.01437i	−0.00424+0.00231i	−0.00753+0.00321i	−0.01341+0.00458i	−0.00801+0.00279i	−0.01333+0.00434i	−0.03815+0.00774i
	0.3	−0.00713+0.00307i	−0.01823+0.00615i	−0.10152+0.01233i	−0.00438+0.00223i	−0.00627+0.00331i	−0.01656+0.00495i	−0.00800+0.00277i	−0.01421+0.00440i	−0.05712+0.00906i
	0.4	−0.00661+0.00294i	−0.01583+0.00476i	−0.06128+0.00971i	−0.00456+0.00235i	−0.00933+0.00344i	−0.02226+0.00556i	−0.00583+0.00274i	−0.01490+0.00443i	−0.09236+0.01077i
	0.5	−0.00601+0.00279i	−0.01333+0.00434i	−0.03815+0.00774i	−0.00474+0.00237i	−0.01064+0.00360i	−0.03282+0.00948i	−0.00577+0.00267i	−0.01493+0.00436i	−0.11895+0.01185i
	0.6	−0.00540+0.00264i	−0.01105+0.00393i	−0.02561+0.00635i	−0.00489+0.00238i	−0.01204+0.00376i	−0.05316+0.00792i	−0.00551+0.00260i	−0.01406+0.00419i	−0.09083+0.01038i
	0.7	−0.00480+0.00247i	−0.00911+0.00356i	−0.01809+0.00534i	−0.00496+0.00237i	−0.01312+0.00386i	−0.08635+0.00990i	−0.00516+0.00249i	−0.01240+0.00392i	−0.06388+0.00616i
	0.8	−0.00424+0.00231i	−0.00753+0.00321i	−0.01341+0.00458i	−0.00493+0.00223i	−0.01347+0.00386i	−0.11600+0.01110i	−0.00474+0.00237i	−0.01064+0.00360i	−0.03362+0.00448i
	0.9	−0.00373+0.00216i	−0.00625+0.00290i	−0.01028+0.00398i	−0.00478+0.00219i	−0.01280+0.00374i	−0.08896+0.00974i	−0.00429+0.00224i	−0.00889+0.00338i	−0.02156+0.00531i